THE PENNSYLVANIA STATE UNIVERSITY
SCHREYER HONORS COLLEGE

DEPARTMENT OF MATHEMATICS

PREDICTING EFFECTIVENESS OF ON-DEMAND PRE-EXPOSURE PROPHYLAXIS TO PREVENT HIV

OLGA DORABIALA
SPRING 2018

A thesis
submitted in partial fulfillment
of the requirements
for a baccalaureate degree
in Mathematics
with honors in Mathematics

Reviewed and approved* by the following:

Jessica M. Conway
Assistant Professor of Mathematics
Thesis Supervisor

Diane Henderson
Professor of Mathematics
Honors Adviser

*Signatures are on file in the Schreyer Honors College.

Abstract

An important strategy for preventing HIV infection involves taking a drug in case of exposure. Continuous, daily dosing of Truvada, an anti-retroviral HIV drug, with the first dose administered a full month before the initial high-risk incident, is the current CDC recommendation for preventing infection through pre-exposure prophlyaxis (PrEP) [1]. However, the IPERGAY study showed that taking only three doses - one before and two following exposure to HIV - may prevent HIV infection almost as effectively as continuous dosing, with the added benefit of smaller quantity of drugs being administered. This is called "on-demand PrEP" [2]. For this latter strategy, uncertainty exists around the optimum time to start treatment as well as how many doses to take. To address this question, we developed and analyzed a mathematical model of early infection and pre-exposure prophylaxis of HIV infection based on virus dynamics and the pharmacokinetics and pharmacodynamics of Truvada. We ran simulations and analyzed the results in order to come up with predictions and recommendations on the best strategies for disease prevention with regards to when to start and stop treatment and the frequency of doses, within the range one is safely permitted to take. We show that PrEP is likely an effective method for preventing infection and provide more narrow guidelines for a dosing schedule than those used in the IPERGAY study.

Table of Contents

List of Figures

List of Tables

Acknowledgements

I would like to thank Dr. Jessica Conway for her guidance, patience, and direction throughout this process and my time at the Pennsylvania State University. Without her support, my undergraduate experience would have been very different, and I may have never discovered my passion for this area of research. Her continuous encouragement and counsel have helped me get this far and have given me a strong foundation for my future.

Chapter 1

Introduction

1.1 Introduction

HIV is a virus that leads to severe impairment of the immune system, leaving infected individuals prey to opportunistic infections [5]. The disease progression is characterized by three phases, which can be seen in Figure 1.1. The first phase occurs after initial exposure to virus and is marked by the development of high viral loads and flu-like symptoms. In Figure 1.1, this phase occurs between 0 to 9 weeks. We note that the graph does not provide any information until about three weeks, and this is because the earliest stage of HIV infection is not well understood. During the second phase, which can last anywhere from a few months to a few years, the patient is largely asymptomatic, but virus continues to replicate and the population of $CD4^+$ T cells in the body slowly decreases. The final phase is the development of AIDS, which occurs when the population of $CD4^+$ T cells is so low that the patient's immune system is potentially fatally compromised [5].

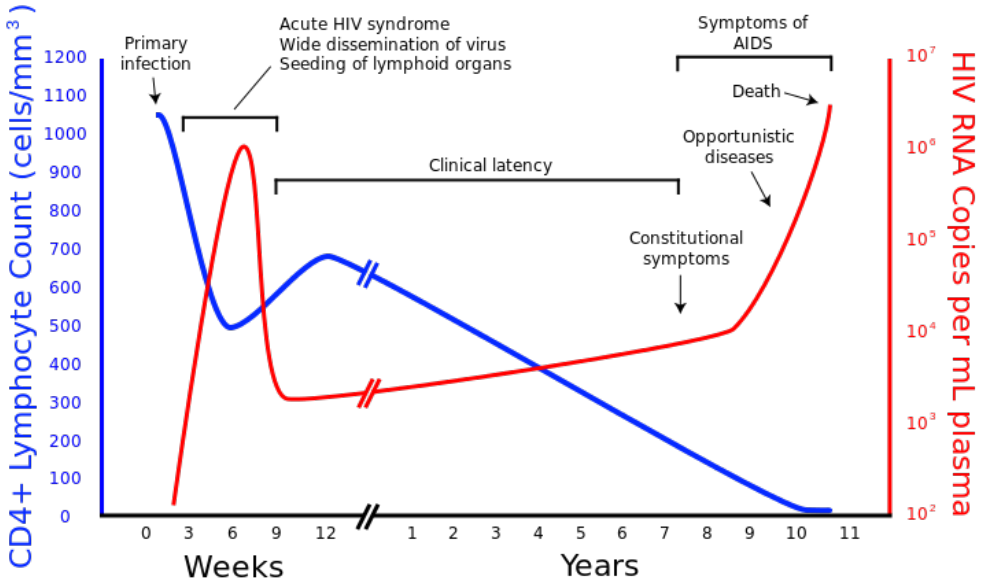

Figure 1.1: **Life Cycle of Untreated HIV** A simplified graph of the relationship between HIV Virus and $CD4^+$ T cells in the body over the course of an untreated HIV infection (Wikimedia Commons, public domain image).

In this paper, we will be focused on the first phase of early viral infection, immediately following exposure to virus and before development of detectable infection. This is the part of Figure 1.1 for which there is no information. The transmission probability of HIV per sexual or blood

exposure is extremely rare, at about $10^{-3} - 10^{-2}$ per sex act, and when infection does occur, it is usually from a single founder strain [3]. Experimentally, it is difficult to study this phase of HIV, particularly before detectable levels of infection are reached, due to the there being such a low viral load and a very small number of infected cells in both humans and animals during the time immediately following exposure.

Although data on the early viral dynamics is hard to obtain, it has been shown that HIV infection can be effectively controlled early on through the use of anti-retroviral drug therapy, taken either as post- or pre-exposure prophylaxis (PEP and PrEP, respectively) [6] [1]. PEP therapy begins as soon as possible following exposure, whereas PrEP focuses on taking anti-retroviral treatments (ARTs) before anticipated exposure. Both treatments aim to eliminate the virus before infection can occur [1].

Current guidelines from the Center for Disease Control and Prevention (CDC) for postexposure prophylaxis (PEP) recommend that care should be sought within 72 hours following HIV exposure and then high doses of three anti-retroviral drugs should be administered for 28 days thereafter [7]. Occupational PEP for workers who are consistently exposed to virus has been proven effective, with a case-control study of HIV infection and transmission among health care workers showing that occupational PEP achieved an 81% reduction in the odds of HIV transmission [6]. Due to ethical and logistical challenges, no randomized, placebo-controlled trials have been carried out to directly test the effectiveness of non-occupational PEP. Instead, case reports and observational studies have been used, but with no conclusive results [7].

Extending the notion of ARTs for prevention, pre-exposure prophylaxis (PrEP) was developed with the aim of providing treatment before exposure even occurred. Clinical trials of PrEP have been carried out with variable success [8] [9] [10]. The time from initiation of daily doses of antiretroviral drugs to maximal protection against infection is currently unknown, especially since every drug has a different protective contribution. As a result, the CDC currently suggests continuous, daily dosing of two HIV antiretroviral drugs in the form of one pill known as Truvada in order to prevent infection [1]. However, the recent clinal IPERGAY trial suggests that treatment does

not have to be administered continuously, but can rather be ”on-demand” and event-driven. This means that one could take a drug depending on when he or she knew exposure would occur. The IPERGAY study found when that therapy was administered within 24 hours before anticipated exposure, 24 hours after exposure, and 48 hours after exposure, the risk of HIV infection was reduced by 86% [2]. In this dissertation, we focus on PrEP.

Here, we use mathematical models of early HIV infection to better inform the use of pre-exposure prophylaxis treatments. Since infection following exposure is a rare event, we focus on a stochastic model formulation based on a continuous-time branching processes, which allows us to calculate the probability of infection by a single founder virus. The novelty of our model is the incorporation of in-tissue pharmacokinetic and pharmacodynamic dynamis in the context of PrEP to provide more accurate representations of drug uptake and effect.

In the following sections, we describe our model and derive expressions for the probabilities of extinction as a function of time. Our methodology allows us to calculate these probabilities, even when the rates in our model are time-dependent, thereby making it possible to explore the impact of various pre-exposure prophylaxis regimens on the probability of extinction. We start with therapy that assumes a constant drug efficacy and then move to explore drug efficacies that differ with time. We obtain these time-dependent efficacies through the use of a pharmacokinetic and pharmacodynamic compartmental model of the PrEP drug Truvada. We conclude with a discussion of our results with respect to effective dosing schedules and ideas for possible future work.

Chapter 2

A Stochastic Model

2.1 Introduction

We present results from two models of early HIV infection. The first will be a simple model that captures only the interactions between productively infected cells and virus, while the second will be extended to include the behavior of non-productively infected cells, which do not produce virus, and incompetent virus, which is unable to infect other cells. Using these models, we explore the dynamics of HIV with the ultimate goal of obtaining the probability of extinction of an infection. Since early infection can be thought of as a stochastic process, we begin with the typical approach of using SSA to investigate HIV dynamics, but conclude that this formulation is inadequate for our problem. We then derive analytical results of extinction for our simple model using a continuous-time branching process approach and show that this formulation is superior in its ability to capture the time-dependent behavior of various components of our model. The analysis of the extended model is essentially the same, but the formulas are a lot longer.

2.2 The Simplest Model

The schematic of our simple model is shown below in Figure 2.1. Cells are infected by virus, V, at a rate of kT, which captures the rate at which virus finds uninfected cells, the rate of virus entry, and the probability of successful infection. Infected cells, I, produce a viral burst size, N, of virus before dying at rate δ. The viral production rate, p, is calculated as $N\delta$. Virus clears at a rate c. Thus the average lifetime of an infected cell is $\frac{1}{\delta}$, and the average lifetime of virus is $\frac{1}{c}$. Finally, unlike standard virus dynamic models, we take the population of uninfected cells T as a constant value, since the number is large and very few cells are infected at the early stage of infection. [11].

This model is referred to as the "continuous production" model, because once a cell is infected it produces virus continuously throughout its life. Another related version of this model is the "burst model" in which we assume that an infected cell releases all of its virus in a single burst that occurs at the time of its death [3]. The true behavior of virus production is not clear, but for the

rest of this section, we focus on the "continuous production" model.

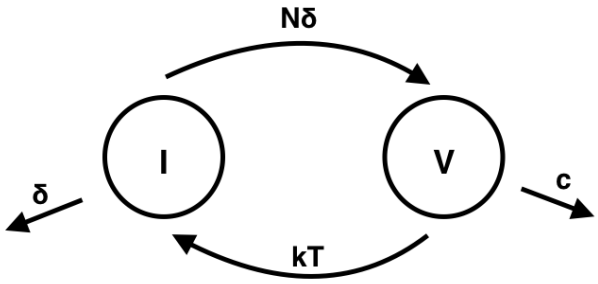

Figure 2.1: **Continuous Production Model Schematic.** A simple compartmental model of early HIV infection. I represents infected cells, which are produced by virus, V, at rate kT and produce virus at rate $N\delta$. Virus clears at rate c, and infected cells clear at rate δ.

The mean-field kinetics of this model can be written as follows, where V and I are the concentrations of virus and infected cells, respectively.

$$\frac{dV}{dt} = -(c + kT)V + N\delta I \tag{2.1}$$

$$\frac{dI}{dt} = kTV - \delta I \tag{2.2}$$

The origin (V=I=0) is clearly a steady-state of the system. It is linearly stable if the basic reproductive ratio $R_0 < 1$. We calculate the value of R_0 in Equation 2.3 by calculating the determinant of the previous linear system.

$$R_0 = \frac{NkT}{kT + c} \tag{2.3}$$

R_0 is a term used to predict whether or not a virus can grow and establish infection. It is defined as the number of newly infected cells that arise from any one infected cell when almost all cells are uninfected [5]. If $R_0 < 1$, then the infection will die out, since on average every infected cell will produce less than one other infected cell. On the other hand if $R_0 > 1$, exposure to virus may lead to persistent infection since on average every infected cell will produce more than one newly infected cell.

Since the earliest events in infection are stochastic, whether exposure to virus leads to infection or not is a matter of chance [3]. Variation in outcomes can be considered as random biological or

statistical variation, and continuous differential equation based models are inadequate for capturing this behavior [11]. This is because these mean field models always show growth when $R_0 > 1$. In order to address questions of risk when populations of infected and viral cells are small, stochastic simulations are used to explore the early dynamics of HIV infection.

2.3 Investigation via SSA

A unique characteristic of HIV is that not much is known about what occurs during early infection. This period of time is referred to as the "eclipse" phase, during which the virus remains below the limit of detectability of current assays. In Figure 1.1, this is the period of time between 0 to 3 weeks before we know anything about the presence of HIV virus. Therefore, we use stochastic simulation to explore this period of time.

First, we reproduce the results of a stochastic model introduced by Pearson et al. that studied the duration of the eclipse phase using the stochastic simulation ("Gillespie") algorithm [3][12]. The paper found that on average, the length of the eclipse phase is 1.78 days in instances where one viron leads to infection. When extinction occurs, however, it only takes an average of .08 days for the initial infection introduced by one viron to clear. Persistent infection is assumed to be when the number of infected cells reaches 32, since beyond that point the probability of stochastic extinction is on the order of 10^{-17} [3]. We reproduce these results in Figures 2.2 and 2.3 by running stochastic simulations of HIV infection initiated by one viron in order to visualize the behavior of the eclipse phase. For illustrative purposes, we use the following parameters: $N = 10$, $kT = 10$ day^{-1}, $\delta = 1$ day^{-1}, and $c = 20$ day^{-1} [3].

From Figures 2.2 (b) and 2.3 (b), we see that whether a realization leads to infection or extinction is quite random. For realizations leading to persistent infection, the initial virus quickly infects a cell, which then rapidly begins to produce more virons. Virons are cleared and produced stochastically, leading to fluctuation in their quantity. For realizations leading to extinction, both the number of infected cells and virus remain small until the infection is extinguished.

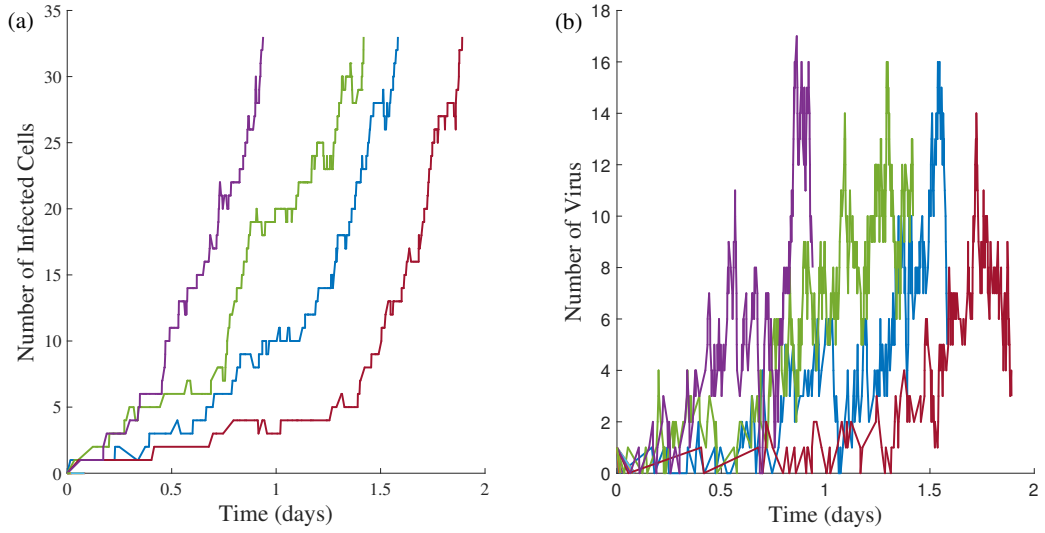

Figure 2.2: **Stochastic Simulation of HIV Eclipse Phase Part 1.** These graphs show the various outcomes of twelve simulations of HIV infection following exposure to one virus. (a) shows the fluctuation in the number of infected cells over time, while (b) shows how the number of virus varies over time. Here, only four of the twelve simulations result in persistent infection. We use the following parameters: $N = 10$, $kT = 10$ day^{-1}, $\delta = 1$ day^{-1}, and $c = 20$ day^{-1} [3].

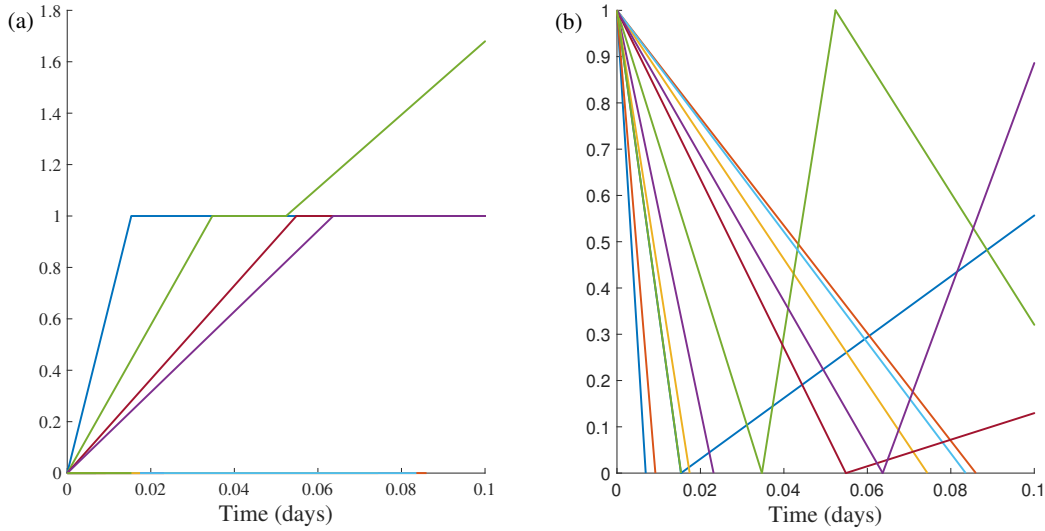

Figure 2.3: **Stochastic Simulation of HIV Eclipse Phase Part 2.** These graphs show the outcomes of twelve simulations of HIV infection following exposure to one virus. They are zoomed in to highlight the behavior when the simulations lead to extinction. We use the following parameters: $N = 10$, $kT = 10$ day^{-1}, $\delta = 1$ day^{-1}, and $c = 20$ day^{-1} [3].

To truly be able to analyze this model and provide reasonable results, Pearson et. al ran a total of 306,592 simulations [3]. From these simulations, they concluded that the probability of viral ex-

tinction was 76.7% and the probability of infected cell clearance was 30 %. Clearly, this method is computationally demanding, especially if one were to consider different parameter sets. Therefore, instead of running hundreds of thousands of simulations, we use on a multi-type continuous-time branching process model, which can be thought of as a collection of simple birth and death processes [13]. We ultimately use this formulation to derive probability distribution functions for viral load as a function of time and use these functions to directly obtain the cumulative probability of extinction. We find that we can recover the same probabilities derived by Pearson et. al's simulation using our approach.

2.4 Backwards Chapman Kolmogorov Differential Equation

At any time t, let there be n infected cells and v virus. After a waiting time h, the process can move to one of a handful of neighboring states, such as $(n+1, v)$, in which the number of infected cells increases by one, but the number of virus remains the same. The resulting "birth and death processes" can then be considered the continuous time analogues of random walks [13]. We assume that $X(t)$ is a Markov process on every state, and that it's transition probabilities are stationary. Then the probability of moving from initial state (n_0, v_0) to state (n, v), in time h are represented as follows.

$$P_{n,v;n_0,v_0}(t) = Pr\{X(t+h) = n, v | X(h) = n_0, v_0\} \tag{2.4}$$

Furthermore, all of the transition probabilities of the simple HIV infection model in Figure 2.1 satisfy the dynamics given in Table 2.1.

As previously mentioned, we aim to derive the probability of extinction $p_{ext}(t) = P_{0,0,n_0,v_0}$. We find this probability, as well as that for all other transitions, by deriving equations for the probability generating function using the Backwards Chapman Kolmogorov Differential Equation.

Using the Markovian property of the process, the Backwards Chapman-Kolmogorov equation states that in order to move from state n_0, v_0 to n, v in time t, the process first moves to some state

Table 2.1: Reactions

$I \to I + V$	$P_{n_0,v_0+1;n_0,v_0}(h) = n_0 ph + \sigma(h)$
$I \to \varnothing$	$P_{n_0-1,v;n_0,v_0}(h) = n_0 \delta h + \sigma(h)$
$V \to I$	$P_{n_0+1,v_0-1;n_0,v_0}(h) = v_0 kTh + \sigma(h)$
$V \to \varnothing$	$P_{n_0,v_0-1;n_0,v_0}(h) = v_0 ch + \sigma(h)$
nothing changes	$P_{n_0,v_0;n_0,v_0}(h) = 1 - n_0 ph - v_0 kTh - v_0 ch - n_0 \delta h + \sigma(h)$

i, j in time $\tau - h$ and then from i, j to n, v in the remaining time τ.

$$P_{n,v;n_0,v_0}(t;\tau - h) = \sum_{i=0}^{\infty}\sum_{j=0}^{\infty} P_{n,v;i,j}(t,\tau) P_{i,j;n_0,v_0}(\tau, \tau - h) \tag{2.5}$$

For small h, we can write this probability for our model as follows,

$$\begin{aligned} P_{n,v;n_0,v_0}(t,\tau - h) &= \sum_{i=0}^{\infty}\sum_{j=0}^{\infty} P_{n,v;i,j}(t,\tau) P_{i,j;n_0,v_0}(\tau,\tau - h) \\ &= P_{n,v;n_0-1,v_0}(t,\tau) P_{n_0-1,v_0;n_0,v_0}(\tau,\tau - h) \\ &\quad + P_{n,v;n_0+1,v_0-1}(t,\tau) P_{n_0+1,v_0-1;n_0,v_0}(\tau,\tau - h) \\ &\quad + P_{n,v;n_0,v_0-1}(t,\tau) P_{n_0,v_0-1;n_0,v_0}(\tau,\tau - h) \\ &\quad + P_{n,v;n_0,v_0+1}(t,\tau) P_{n_0,v_0+1;n_0,v_0}(\tau,\tau - h) \\ &\quad + P_{n,v;n_0,v_0}(t,\tau) P_{n_0,v_0;n_0,v_0}(\tau,\tau - h) + \sum_i \sum_j P_{n,v;i,j}(t,\tau) P_{i,j;n_0,v_0}(\tau,\tau - h) \end{aligned} \tag{2.6}$$

Looking at the last term in Equation 2.6 and substituting the transition probabilities from Table 2.1, we note that,

$$\begin{aligned} \sum_i \sum_j P_{n,v;i,j}(t,\tau) P_{i,j,n_0,v_0}(\tau,\tau - h) &\le P_{i,j,n_0,v_0}(\tau,\tau - h) \\ &= 1 - [nph + \sigma(h) + n_0\delta h + \sigma(h) + v_0 kT(\tau - h)h \\ &\qquad + \sigma(h) + v_0 ch + \sigma(h) \\ &\qquad + (1 - nph - vch - n\delta h - vkT(\tau - h)h + \sigma(h)] \\ &= \sigma(h) \end{aligned} \tag{2.7}$$

Then we can simplify the original sum as follows,

$$\begin{aligned} P_{n,v;n_0,v_0}(t;\tau - h) &= n_0 \delta h P_{n,v;n_0-1,v_0}(t,\tau) + v_0 kTh P_{n,v;n_0+1,v_0-1}(t,\tau) \\ &\quad + v_0 ch P_{n,v;n_0,v_0-1}(t,\tau) + n_0 ph P_{n,v;n_0,v_0+1}(t,\tau) \\ &\quad + [1 - h(n_0 p + v_0 c + n_0\delta + v_0 kT)] P_{n,v;n_0,v_0}(t,\tau) + \sigma(h) \end{aligned} \tag{2.8}$$

Transposing the term $P_{n,v;n_0,v_0}$ to the left-hand side and dividing the equation by h, we obtain, after letting $h \to 0$.

$$\begin{aligned}\frac{dP_{n,v;n_0,v_0}(t,\tau)}{d\tau} &= n_0\delta P_{n,v;n_0-1,v_0}(t,\tau) + v_0 kT(\tau) P_{n,v;n_0+1,v_0-1}(t,\tau) + v_0 c P_{n,v;n_0,v_0-1}(t,\tau) \\ &\quad + n_0 p P_{n,v;n_0,v_0+1}(t,\tau) - (n_0 p + v_0 c + n_0\delta + v_0 kT(\tau)) P_{n,v;n_0,v_0}(t)\end{aligned} \tag{2.9}$$

Note that this equation is backwards in time: $\tau : t \to 0$. From here, we define the probability generating function $G_{n_0,v_0}(x,y,t,\tau)$, which will allow us to calculate any probability, by multiplying Equation 2.9 by $x^n y^v$ and summing over n and v.

$$G_{n_0,v_0}(x,y,t,\tau) = \sum_{n,v=0}^{\infty} P_{n,v,n_0,v_0}(t,\tau) x^n y^v \tag{2.10}$$

This leads us to the obtain the following equation and terminal conditions.

$$\begin{aligned}\frac{\partial G_{n_0,v_0}}{\partial \tau} &= -n_0[\delta G_{n_0-1,v_0} + pG_{n_0,v_0+1} - (p+\delta)G_{n_0,v_0}] \\ &\quad - v_0[kTG_{n_0+1,v_0-1} + cG_{n_0,v_0-1} - (c+kT)G_{n_0,v_0}]\end{aligned} \tag{2.11}$$

Terminal Condition: $G_{n_0,v_0}(x,y;t,t) = \sum_{n=0}^{\infty}\sum_{j=0}^{\infty} P_{n,v;n_0,v_0}(t,t)x^n y^v = \sum_{x=0}^{\infty}\sum_{v=0}^{\infty}\delta_{n,v;n_0,v_0}x^n y^v = x^{n_0}y^{v_0}$

This is an infinite dimensional equation, but due to independence can be simplified using the branching property, which states that $G_{n,v} = G_{1,0}^n G_{0,1}^v$. This means that we only need the probability generating function differential starting with a single infected cell, $G_{1,0}$, and starting with a single virus $G_{0,1}$.

$$\frac{\partial G_{1,0}}{\partial t} = -n_0\Big[\delta G_{0,0} + pG_{1,1} - (p+\delta)G_{1,0}\Big] = -n_0\Big[\delta + pG_{1,0}G_{0,1} - (p+\delta)G_{1,0}\Big] = -\delta - pG_{1,0}G_{0,1} + (p+\delta)G_{1,0} \tag{2.12}$$

$$\frac{\partial G_{0,1}}{\partial t} = -v_0\Big[kTG_{1,0} + cG_{0,0} - (c+kT)G_{0,1}\Big] = -v_0\Big[kTG_{1,0} + c - (c+kT)G_{0,1}\Big] = -kTG_{1,0} - c + (kT+c)G_{0,1} \tag{2.13}$$

We want to solve for the clearance probabilities, or the probabilities that a process initiated either by a single viron or a single infected cell results in extinction. We recall that $p_{ext}(t) = P_{0,0,n_0,v_0} = G_{n_0,v_0}(0,0;t,0)$ and that $p_{ext}^{\infty} = \lim_{t\to\infty} G_{n_0,v_0}(0,0;t,0)$. If all of the rates are constant, then the probabilities of extinction are simply the fixed point of the system where $\frac{\delta G_{1,0}}{\delta t} = 0$ $\frac{\delta G_{0,1}}{\delta t} = 0$. Solving the system, we obtain a pair of algebraic equations. Let $p_I = G_{1,0}$ and $p_V = G_{0,1}$. Also, recall that $p = N\delta$.

$$p_I = \frac{1}{N+1} + \frac{N}{N+1} p_I p_V \tag{2.14}$$

$$p_V = \gamma p_I + (1-\gamma) \tag{2.15}$$

Since probabilities need to be less than or equal to one, we obtain the following solution. Equations 2.16 and 2.17 are our analytic expressions for p_V and p_I under a continuous viral production assumption. These quantities are identical to those derived using recurrsion in [12]. In chapters 3 and 4, we will relax the assumption that the rates are constant and instead vary them with time. Thus, finding the fixed point of the system will no longer be an option, and we will instead be forced to use our machinery, rather than stochastic simulation, to tackle the problem.

$$p_I = min(1, \frac{1}{N\delta} = \frac{1}{R_0}) \tag{2.16}$$

$$p_V = min(1, 1 - \frac{R_0 - 1}{N}) \tag{2.17}$$

2.5 A More Detailed Model for Early HIV Infection

For the predictions that follow, we use a more detailed model, which encompasses four compartments: productively infected cells, I_1, productively incompetent cells in the eclipse phase, I_2, virus, V, and incompetent virus, W. The schematic is shown in Figure 2.4 and the parameters are displayed in Table 2.2. All of the parameters are the same as in the previous model, with the introduction of s, the rate at which infected cells leave the eclipse phase, and Q_a, the fraction of

replication-competent virus [14] [15].

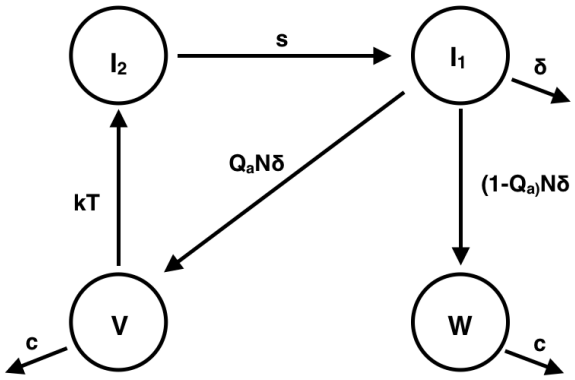

Figure 2.4: **Continuous Production Model Schematic.** A more detailed compartmental model of early HIV infection. I_1 represents productively infected cells, I_2, represents productively incompetent cells in the eclipse phase, V represents virus, and W represents incompetent virus. Virus infects cells at rate kT and infected cells produce virus at rate $Q_a N\delta$. Infected cells leave the eclipse phase at rate s. Virus and incompetent virus clear at rate c, while productively infected cells clear at rate δ.

Let n be the number of productively infected cells, m the number of unproductively infected cells, and v the number of replication competent virus at time t. We neglect unproductive virus, W, since it makes no contribution to the spread of infection [14]. Then, following the same process as before, we again derive the backwards Chapman-Kolmogorov differential equation for the model.

$$\begin{aligned}\frac{dP_{n,m,v;n_0,m_0,v_0}(t,\tau)}{d\tau} &= -sm_0P_{n,m,v;n_0+1,m_0-1,v_0}(t,\tau) - \delta n_0 P_{n,m,v;n_0-1,m,v}(t,\tau) \\ &\quad - Q_a p n_0 P_{n,m,v;n_0,m_0,v_0+1} - cv_0 P_{n,m,v;n_0,v_0,v_0-1} - kTv_0 P_{n,m,v;n_0,m_0+1,v_0-1} \\ &\quad + [sm_0 + (\delta + Q_a p)n_0 + (c+kT)v_0]P_{n,m,v,n_0,m_0,v_0}\end{aligned} \tag{2.18}$$

Defining the corresponding probability generating function

$$G_{n_0,m_0,v_0} = \sum_{n=0}^{\infty}\sum_{m=0}^{\infty}\sum_{v=0}^{\infty} P_{n,m,v;n_0,m_0,v_0}(t,\tau)x^n z^m y^v\,, \tag{2.19}$$

we derive the following differential equations for the probability generating function,

$$\frac{\delta G_{1,0,0}}{\delta t} = -\delta(1 - G_{1,0,0}) - Q_a p G_{1,0,0}(G_{0,1,0} - 1) \tag{2.20}$$

$$\frac{\delta G_{0,1,0}}{\delta t} = -kTG_{0,0,1} - c + (c + kT)G_{0,1,0} \tag{2.21}$$

$$\frac{\delta G_{0,0,1}}{\delta t} = -s(G_{1,0,0} - G_{0,0,1}) \tag{2.22}$$

Then using the branching property, $G = G_{1,0,0}^{n_1} G_{0,1,0}^{n_2} G_{0,0,1}^{v}$, we compute the probabilities of extinction starting with a single infected cell, p_I, or a single virus, p_V to obtain

$$p_I = \frac{c + kT}{NQ_a kT} \tag{2.23}$$

$$p_V = \frac{1}{NQ_a} + 1 - \frac{kT}{kT + c} \tag{2.24}$$

Observe that the eclipse phase, $\frac{1}{s}$ does not affect these probabilities; it will only delay time to extinction or infection detection. However, the fraction of competent virus that is produced, Q_a. greatly enhances the probabilities of extinction, since only competent virus can spread infection.

2.6 Parameters

The baseline parameters for our model are given in Table 2.2. Current estimates suggest that the death rate of infected cells $\delta = 1$ day^{-1} [16]. The best estimate for the viral burst size N comes from an experiment in which cells infected with SIV, the analogue to HIV in primates, were placed into uninfected rhesus macaques and the viral load data was monitored. Taking into account the rate of clearance, the burst size was found to be approximately 5000 virons per infected cell. [16][17]. Since we know that the viron production rate $p = N\delta$, we can say $p = 5000$ virons per day. In the blood, the clearance rate c is estimated to be 23 days^{-1} [16]. The rate at which infected cells leave the eclipse phase is taken to be $s = 1$ day^{-1}. The fraction of replication-competent virus, Q_a is taken to be 10^{-2} [14][18]. This is a conservative estimate, as some estimates have the fraction as low as 10^{-4}.

The infection rate kT cannot be calculated directly, and is instead estimated using our expression involving the basic reproductive ratio R_0. In the extended model, $R_0 = \frac{NQ_a kT}{c+kT}$, and we adjust our computation of kT accordingly. Usually, estimates of R_0 are obtained from small data samples collected primarily near or after peak viral load. Instead, we obtain our estimate of R_0 from a paper

by Ribeiro et. al, which was able to analyze early viral load data from 47 patients before virus was even detectable [19]. We averaged the basic reproductive ratios for each patient over all patients to obtain a mean value of 2.70.

Table 2.2: More Complicated Model Parameters

Paramater	Description	Estimate	Source
δ	Death rate of infected cells	1 day^{-1}	[16]
N	Viral Burst Size	5000 virons per infected cell	[16, 17]
p	Viron production rate	5000 day^{-1}	see text
c	Viron Clearance rate	23 day^{-1}	[16]
R_0	Basic Reproductive Ratio	2.70	[19]
kT	Infection rate	1.31	see text
s	Rate at which infected cells leave the eclipse phase	1 day^{-1}	[15]
Q_a	Fraction of replication competent virus	10^{-2}	[14][18]

Table 2.2 provides baseline parameters for our early-HIV infection model shown schematically in Fig. 2.4. Using these parameters, the probability that infection goes extinct when initiated with one viron is 99.66% and the probability of extinction for infection initiated with one infected cell is 37.04%. In Chapters 3 and 4 we use the model and parametrization, extended to include antiretroviral drug dynamics, to investigate PrEP to prevent infection.

2.7 Conclusion

In Chapter 2, we introduced our model of early HIV infection. We began with a simplified version that we described using mean-field kinetics. We concluded that a continuous differential equation based model is inadequate for capturing the stochastic nature of early infection events and instead turned to stochastic simulation to explore the dynamics of infection. We concluded that this method was computationally inefficient and found that we could extract the same probabilities of extinction through the use of a more efficient, continuous-time branching process model. Using the Backwards Chapman Kolmogorov Differential Equation, we derived probability distribution functions for viral load as a function of time and used these functions to directly obtain the cu-

mulative probability of extinction. We then repeated this process for our extended model of early HIV infection, which we will be using henceforth. Our formulation is essential, as it allows us to relax the assumption that rates must be constant in time, and in the following chapters we will be using time-dependent rates to investigate pre-exposure prophylaxis treatments for the prevention of infection.

Chapter 3

Modeling Pre-exposure Prophyaxis Effectiveness

3.1 Introduction

Our aim is to investigate the effectiveness of a drug regimen to prevent HIV in advance of exposure through pre-exposure prophylaxis (PrEP). In the present chapter, we assume constant drug efficacy, thereby creating a homogeneous time-branching process, and explore which efficacies provide the greatest increase in the probability of extinction in the context of to two different types of therapy.

3.2 HIV Treatments

Two of the most commonly used forms of antiretroviral drug therapy (ART) for combating the HIV virus are Reverse Transcriptase Inhibitors (RTIs) and Protease Inhibitors (PIs) [5]. RTIs were the first available drugs for treating HIV. They work by inhibiting the reverse transcriptase enzyme in the HIV virus, thereby preventing viral RNA from being copied into DNA, a critical step of the HIV life-cycle. In simple terms, they prevent the infection of new cells. On the other hand, PIs interfere with the maturation of new viruses by binding to HIV Protease and leading to the creation of noninfectious virus [5]. Newer forms of treatment include Fusion Inhibitors (FIs) and Integrase Inhibitors (InIs). Fusion Inhibitors prevent the virus from attaching to and entering the target cell, while Integrase Inhibitors prevent HIV DNA from integrating into the host cell's genome [20]. At the resolution of our model, however, their effects are similar to RTIs [21] [22] . We leave the investigation of these drugs for later study. The issue with HIV drugs in general is that when they are used individually, HIV is almost always able to develop resistance [5]. Therefore, the standard approach to preventing HIV infection is to use some type of combination therapy.

We capture the behavior of various types of antiretroviral drug therapy by representing the drug efficacy of reverse transcriptase inhibitors and protease inhibitors as ϵ_{RTI} and ϵ_{PI}, where $0 \leq \epsilon_{RTI}, \epsilon_{PI} \leq 1$, respectively, and altering the system in Equations 2.20 to 2.22 in the following way,

$$\frac{\delta G_{1,0,0}}{\delta t} = -\delta(1 - G_{1,0,0}) - (1 - \epsilon_{PI})Q_a p G_{1,0,0}(G_{0,1,0} - 1) \tag{3.1}$$

$$\frac{\delta G_{0,1,0}}{\delta t} = -(1 - \epsilon_{RTI})kTG_{0,0,1} - c + (c + kT(1 - \epsilon_{RTI}))G_{0,1,0} \tag{3.2}$$

$$\frac{\delta G_{0,0,1}}{\delta t} = -s(G_{1,0,0} - G_{0,0,1}) \tag{3.3}$$

We note that the rate of infection is reduced by $(1 - \epsilon_{RTI})kT$ and the viral production rate is reduced by $(1 - \epsilon_{PI})Q_a p$. When $\epsilon_{RTI} = 1$, the Reverse Transcriptase Inhibitors are fully effective, and successfully prevent any and all transcription of the HIV virus. Similarly, when $\epsilon_{PI} = 1$, the Protease Inhibitors fully prevent the maturation of virus. The analytic expressions for the probability of extinction are derived using the methods described in Chapter 2 and given in Equations 3.4 and 3.5.

$$p_I = \frac{c + (1 - \epsilon_{RTI})kT}{(1 - \epsilon_{PI})NQ_a(1 - \epsilon_{RTI})kT} \tag{3.4}$$

$$p_V = \frac{1}{(1 - \epsilon_{PI})NQ_a} + 1 - \frac{(1 - \epsilon_{RTI})kT}{(1 - \epsilon_{RTI})kT + c} \tag{3.5}$$

3.3 Results

We aim to evaluate how effectively PrEP enhances the probability of infection extinciton. We recall that without any treatment, our baseline probability for an infection begun with one viron goes to go to extinction is 99.66%. Therefore, we use the percent increase in the probability of extinction, defined in Equation 3.6, to quantify the benefits of antiretroviral drug therapy

$$\% \text{ Increase} = \frac{P_{ext}^{new} - P_{ext}^{old}}{P_{ext}^{new}} \times 100 \tag{3.6}$$

Figure 3.1 shows that the probability of extinction increases as a function of drug efficacy for both RTI and PI therapies, matching intuition on how drugs work. We also note that RTIs are more effective than PIs at equal efficacy.

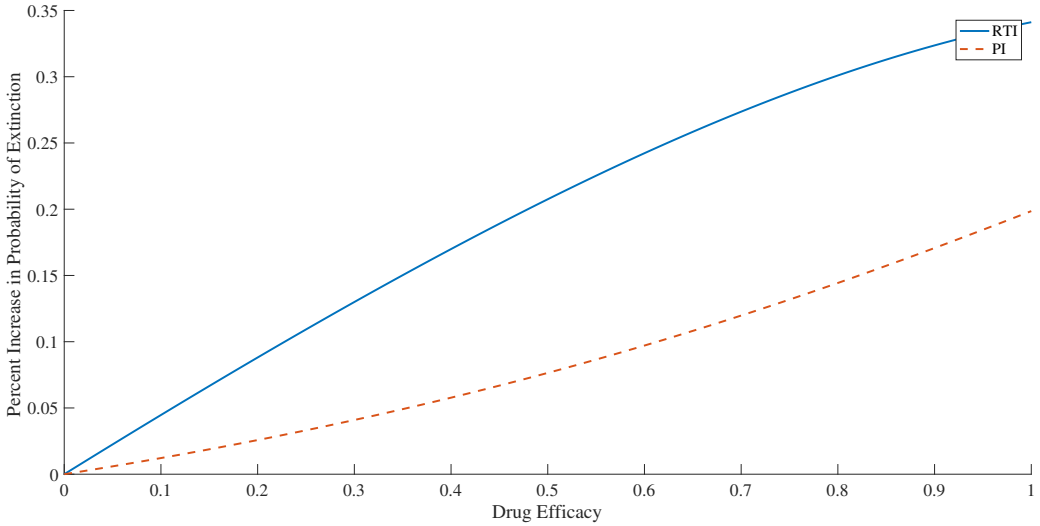

Figure 3.1: **Percent Increase in Probability of Extinction for PrEP Therapy.** We plot drug efficacy for both RTI and PI drugs against the percent increase in the probability of extinction for an infection begun with one viron. Parameters are taken from Table 2.2.

In Figures 3.2-3.5 we investigate the percent change in the probability of extinction with regards to how long therapy is carried out after exposure. We assume a drug to be administered before exposure until it achieves a constant, .80, efficacy. Then, we investigate the impact of PrEP interruption at t_{end} relative to HIV exposure. The equations determining the behavior of $\epsilon_{RTI}(t)$ and $\epsilon_{PI}(t)$ are given in Equation 3.7. Since the efficacies are dependent on time, Equations 3.1-3.3 are not autonomous and the probability of extinction cannot be calculated as the fixed point of the system. Instead, we take $p_V = \lim_{t\to\infty} p_V(t)$ and solve the ordinary differential equations backwards in time with zero terminal conditions.

$$\epsilon_{RTI}(t) = \begin{cases} 0.8 & 0 \leq t \leq t_{end} \\ 0 & t > t_{end} \end{cases} \qquad \epsilon_{PI}(t) = \begin{cases} 0.8 & 0 \leq t \leq t_{end} \\ 0 & t > t_{end} \end{cases} \tag{3.7}$$

Figure 3.2 shows that for drugs with constant efficacies of $\epsilon_{RTI} = .80$ and $\epsilon_{PI} = .80$, respectively, the longer a drug is taken, the greater the percent increase in the probability of extinction, matching intuition. To achieve within .01 of the maximum enhancement relative to p_V, treatment should be carried out for 8.9 days using RTIs or 14.8 days using PIs. We note that much of the

RTIs action is within the first 24 hours, and one must stay on PIs much longer to achieve the same level of protection. This is because RTIs prevent the infection of new cells, which is more effective in early prevention than halting the production of virus.

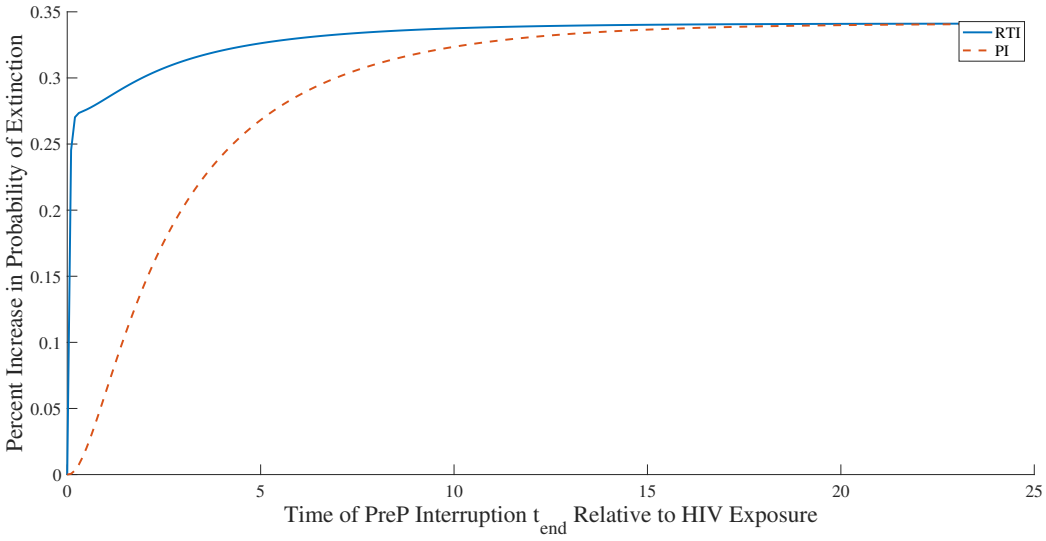

Figure 3.2: **Percent Increase in Probability of Extinction Based on Dosing Schedule.** We plot the time of PrEP interruption of RTI and PI therapy relative to HIV exposure time against the percent increase in the probability of extinction for an infection begun with one viron. The drug efficacies are .80 for both treatments. The Parameters are taken from Table 2.2.

Figures 3.3 and 3.4 are contour plots that show how the percent increase in the probability of extinction depends on drug efficacy and the time until PrEP interruption for RTI and PI treatments, respectively. From these figures, we are able to conclude that for both RTI's and PI's, taking a drug of greater efficacy for a longer amount of time provides the best protection from infection. Overall, the maximum percent increase in the probability of extinction is approached more rapidly for an RTI drug than a PI drug for all drug efficacies.

Next we investigate treatment that uses a combination of both RTI's and PI's. Figure 3.5 shows how the percent change in the probability of extinction varies with differing efficacies of RTI and PI drugs both administered until interruption at 10 days. We note that combination therapy allows for maximum protection to be reached with lower individual drug efficacies. For treatment with an RTI alone that is interrupted at 10 days after exposure, a drug efficacy of about 0.7 is required in order for a probability of extinction within .01 of the maximum to be reached. Similarly, for

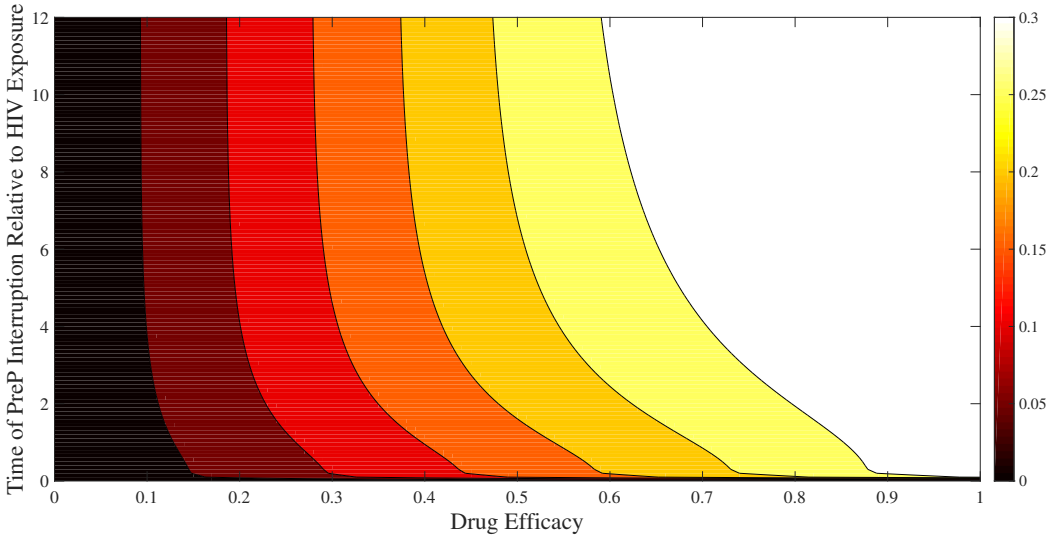

Figure 3.3: **Percent Increase in Probability of Extinction for PrEP using an RTI drug.** Colors and contours indicate the percent increase in probability of extinction for infection begun with one viron for RTI Therapy with varied drug efficacy and dosing schedule. The parameters are taken from Table 2.2

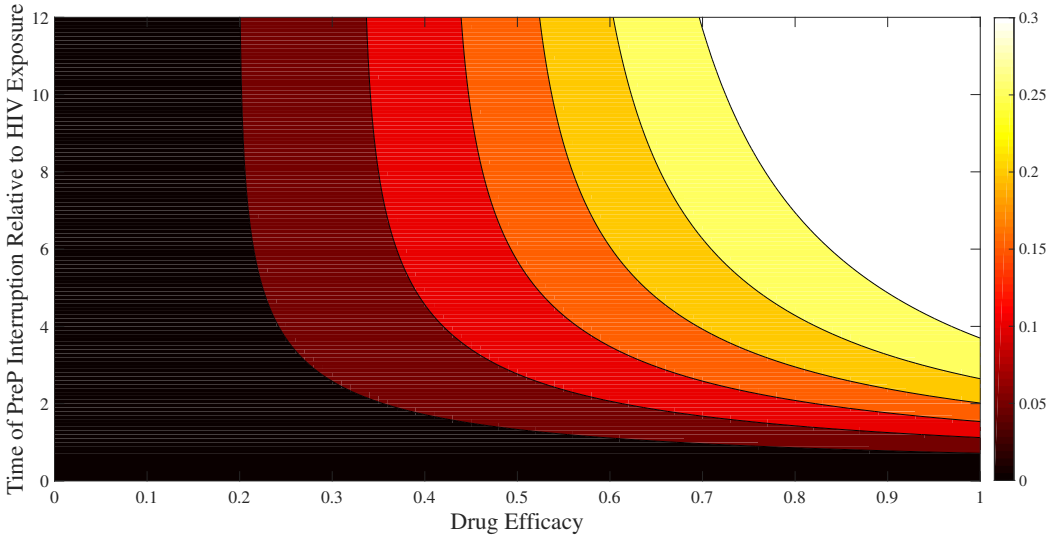

Figure 3.4: **Percent Increase in Probability of Extinction for PrEP using a PI drug.** Colors and contours indicate the percent increase in probability of extinction for infection begun with one viron for PI therapy with varied drug efficacy and dosing schedule. The parameters are taken from Table 2.2

treatment with a PI alone that is interrupted at 10 days after exposure, a drug efficacy of about 0.8 is required in order for a probability of extinction within .01 of the maximum to be reached. On

the other hand, when both drugs are used in combination, the maximum probability of extinction can be approached within .01 of the maximum with efficacies ϵ_{RTI} and ϵ_{PI} much lower than those used in individual drug treatment.

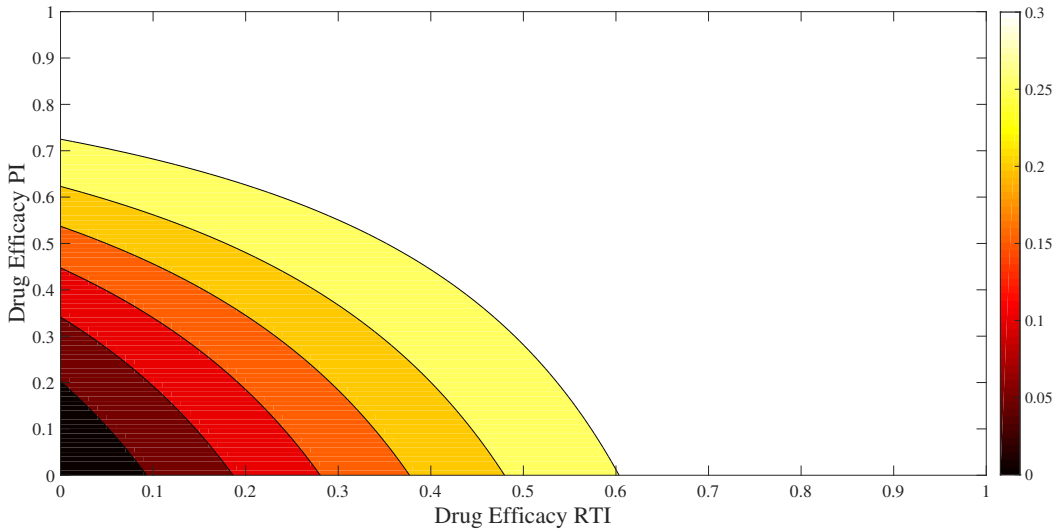

Figure 3.5: **Percent Increase in Probability of Extinction for Combination-therapy PrEP.** Colors and contours indicate the percent increase in probability of extinction for infection begun with one viron for varied drug efficacies for combined therapy using an RTI and a PI. The parameters are taken from Table 2.2

3.4 Conclusion

Overall, we are able to conclude that RTIs are more efficient than PIs in quickly combatting HIV infection. Although treatments with both types of drugs approach within .01 of the maximum probability of extinction as time goes to infinity, RTI treatment does so much faster. Practically speaking, it makes sense to use a drug that requires a shorter duration of treatment due to concerns about side effects and adherence to a schedule. It is therefore no surprise that current PrEP therapy uses Truvada, which is a combination of two RTI drugs [2]. Of course, in this chapter we used a constant drug efficacy, but our goal is to understand "on-demand" PrEP, for which dosing begins only shortly before exposure occurs. We anticipate drug absorption dynamics have an important impact. Therefore, in Chapter 4, we integrate a pharmacokinetic-pharmacodynamic model of Tru-

vada into our model of early HIV dynamics to study the impact of time-dependent drug efficacies on the probability of extinction.

Chapter 4

Modeling On-Demand Pre-exposure Prophylaxis Effectiveness

4.1 Introduction

In the previous chapter, we assumed that drugs retain the same level of efficacy regardless of how long they have been in the system. In reality, drugs ingested orally have to disperse throughout the body and over time become more or less concentrated in various tissues. In order to capture the time-dependent behavior of various HIV drugs, we consider drug pharmacokinetics (PK), which model drug dispersal through the body, and pharmacodynamics (PD), which track how drugs effect the body. Once we calculate a time-dependent efficacy, we integrate it into our model of early HIV infection, thereby creating a time inhomogeneous branching process, and investigate various dosing strategies.

4.2 A Pharmacokinetic/Pharmacodynamic Model

We begin with the PK/PD dynamics of tenofovir disoproxil fumarate (TDF) and emtricitabine (FTC), the two reverse transcriptase inhibitor drugs that make up Truvada, which is FDA approved for PrEP. Specifically, we use the PK/PD model proposed in Cottrell et al. with the ultimate goal of integrating it into our model of early HIV infection [4]. The PK/PD model schematic is reproduced from Cottrell et. al and shown in Figure 4.1. We employ the parametrization found by Cottrell et. al using clinical trial data [4]. All parameters can be found in Table 4.1.

This model tracks the concentrations of TDF and FTC in different tissue compartments following the ingestion of an oral dose. There are eight compartments with 7 gastrointestinal transit compartments, each represented by a linear ordinary differential equation, that ultimately track the concentration of drug in vaginal, cervical, and rectal tissue. Once the drug is ingested, part of it travels through the gut and lands in the rectal tissue. The rest of the drug seeps into the blood plasma, which then distributes to the vaginal, cervical, and rectal tissues. Each tissue leads to its own respective metabolite compartment. We are most interested in how the drug concentrations change in the metabolite compartments, as these are the dynamics that are used to calculate our

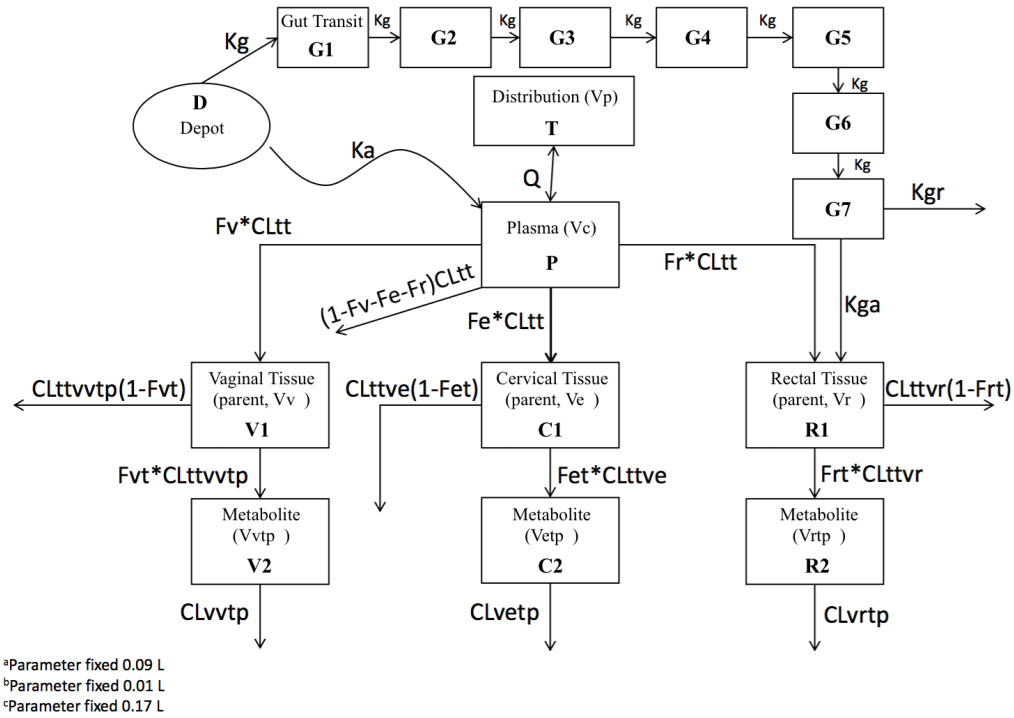

Figure 4.1: **Pharmacokinetic Compartmental Model Schematic. [4]** A 16 compartment model of how drugs travel and are absorbed throughout the body.

final time dependent drug efficacy.

Ingestion is represented in the drug depot by Equation 4.1, where the size of the dose D_0 is multiplied by the sum of delta functions that represent the sudden uptake of drug at dosing times t_n. The remaining fifteen differential equations are given in the system in Equation 4.2.

$$D = D_0 \sum_{n=0}^{N} \delta(t - t_n) \tag{4.1}$$

$$\frac{dG1}{dt} = Kg(D - G1) \qquad \frac{dG5}{dt} = Kg(G4 - G5)$$

$$\frac{dG2}{dt} = Kg(G1 - G2) \qquad \frac{dG6}{dt} = Kg(G5 - G6)$$

$$\frac{dG7}{dt} = KgG6 - KgrG7 - KgaG7$$

$$\frac{dG3}{dt} = Kg(G2 - G3) \qquad \frac{dT}{dt} = Q\frac{P}{Vc} - Q\frac{T}{Vp}$$

$$\frac{dG4}{dt} = Kg(G3 - G4) \qquad \frac{dP}{dt} = KaD - Q\frac{P}{Vc} + Q\frac{T}{Vp} - CLtt\frac{P}{Vc}$$

$$\frac{dR1}{dt} = KgaG7 + FrCLtt\frac{P}{Vc} - CLttvr\frac{R1}{.17} \qquad \frac{dV1}{dt} = FvCltt\frac{P}{Vc} - CLttvvtp\frac{V1}{.09}$$

$$\frac{dR2}{dt} = FrtCl ttvr\frac{R1}{.17} - CLvrtp\frac{R2}{.17} \qquad \frac{dV2}{dt} = FvtCLttvvtp\frac{V1}{.09} - CLvvtp\frac{V2}{.09} \quad (4.2)$$

$$\frac{dC1}{dt} = FeCLtt\frac{P}{Vc} - CLttve\frac{C1}{.01}$$

$$\frac{dC2}{dt} = FetCLttve\frac{C1}{.01} - CLvetp\frac{C2}{.01}$$

Each of these equations has terms representing flow into and out of the compartment. For example, for the Rectal Metabolite compartment, R2, the first term describes the flow of drug into the Rectal Metabolite from the Rectal Tissue. We divide by the volume of the Rectal Tissue compartment, 0.17, in order to correct our units. The second term describes the flow of drug out of the Metabolite and is corrected by the volume of the Rectal Metabolite compartment.

Table 4.1: PK/PD Model Parameters

Parameter	Units	FTC	TFV
Ka	(h^{-1})	0.649	0.863
Vc	(L)	72.3	331
Vp	(L)	122	843
Q	$(\frac{L}{h})$	6.06	142
CLtt	$(\frac{L}{h})$	18.9	58.7
Fv	-	0.00131	0.000079
Fe	-	0.000069	0.000015
Fr	-	0.00401	0.00007
Fvt	-	0.325	0.243
CLttvvtp	$(\frac{L}{h})$	0.0101	0.0111
CLvvtp	$(\frac{L}{h})$	0.0399	0.041
Fet	-	1	0.0292
CLttve	$(\frac{L}{h})$	0.000947	0.00183
CLvetp	$(\frac{L}{h})$	0.0082	0.00207
Frt	-	0.0107	1
CLttvr	$(\frac{L}{h})$	0.0223	0.00477
CLvrtp	$(\frac{L}{h})$	0.647	0.14
Kt	(h^{-1})	0.0724	0.0752
Kga	(h^{-1})	1	0.0589

According to the highly successful IPERGAY study, taking two tablets of Truvada within 24

hours before exposure, one tablet within 24 hours after exposure, and one tablet 24 hours later led to an 86% reduction in risk for HIV infection [2]. We use our PK/PD model in an attempt to recreate these results. First, we investigate how the concentrations of the two components of Truvada, TDF and FTC, change over time in the Vaginal, Cervical, and Rectal Metabolites, respectively. In Figure 4.2, we administer two pills 24 hours prior to exposure, one pill at the time of exposure, and one more 24 hours after. This corresponds to a first dose of 400 mg FTC, followed by two doses of 200 mg each or to a first dose of 600 mg TDF, followed by two doses of 300 mg each. We note that drug uptake is highest in the rectal tissue and metabolite. Furthermore, we capture experimental observations of the preferential uptake of TDF in colorectal tissues and FTC in female genital tract tissues [23]. This has important implications for differences between optimal drug adherence regimens between men and women.

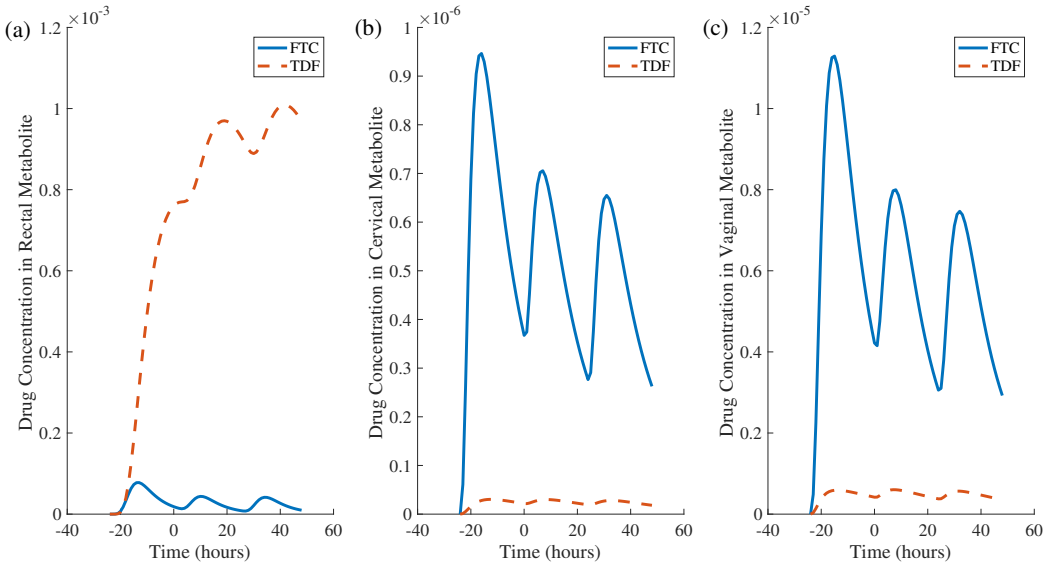

Figure 4.2: **Drug Concentrations in Metabolites.** We show how the concentration of two HIV drugs, FTC and TDF, vary over time in the (a) vaginal, (b) rectal, and (c) cervical metabolites. For FTC, 400 mg are taken 24 hours before exposure, 200 mg at the time of exposure, and 200 mg 24 hours later. For TDF, 600 mg are taken 24 hours before exposure, 300 mg at the time of exposure, and 300 mg 24 hours later. Model parameters can be found in Table 4.1

The concentrations of vaginal, cervical, and rectal metabolite at every time step are used to calculate a drug efficacy ϵ using Equation 4.3. Here, H and EC_{50} are the Hill Slope and 50%

effective concentration parameters, respectively, which are fixed values taken from Cottrell et. al and shown in Table 4.2 [4]. Ψ is a fitted parameter for an efficacy target of 90%. We take $\Psi = 1e^{-11}$.

$$\epsilon = \frac{\frac{TFV}{\Psi \times EC_{50,TFV}} H_{TFV} + \frac{FTC}{\Psi \times EC_{50,FTC}} H_{FTC} + \frac{TFV}{\Psi \times EC_{50,TFV}} H_{TFV} \times \frac{FTC}{\Psi \times EC_{50,FTC}} H_{FTC}}{1 + \frac{TFV}{\Psi \times EC_{50,TFV}} H_{TFV} + \frac{FTC}{\Psi \times EC_{50,FTC}} H_{FTC} + \frac{TFV}{\Psi \times EC_{50,TFV}} H_{TFV} \times \frac{FTC}{\Psi \times EC_{50,FTC}} H_{FTC}} \quad (4.3)$$

Table 4.2: Efficacy Equation Parameters

	EC_{50}	Hill Slope
TFV	311	1.02
FTC	821	1.48

Figures 4.3 shows how drug efficacy varies in the rectal, vaginal, and cervical metabolites, respectively, over time for a combined treatment of 400 mg of FTC and 600 mg of TDF 24 hours before exposure and 200 mg of FTC and 300 mg of TDF at and 24 hours after exposure to HIV. We see that the efficacy increases at each time of dosing, decreases slowly thereafter, and that continuous dosing maintains a high drug efficacy. We also note that drug efficacy is highest in the rectal metabolite.

For the remainder of this chapter, we will focus on the drug efficacy in the rectal metabolite when calculating drug efficacies, since one of the populations most affected by HIV in the USA is men who have sex with men, and unprotected anal intercourse for that population is the most likely route of transmission [1].

4.3 Results of Effectiveness of On-Demand PrEP

We integrate the time dependent drug efficacy that we obtained through the PK/PD model into our original model of early HIV infection and provide recommendations for various dosing schedules. We recall that the IPERGAY study states that a first dose of two pills should be taken prior to exposure, a second dose of one pill should be taken within 24 hours of exposure, and a third dose of one pill should be taken 24 hours later [2].

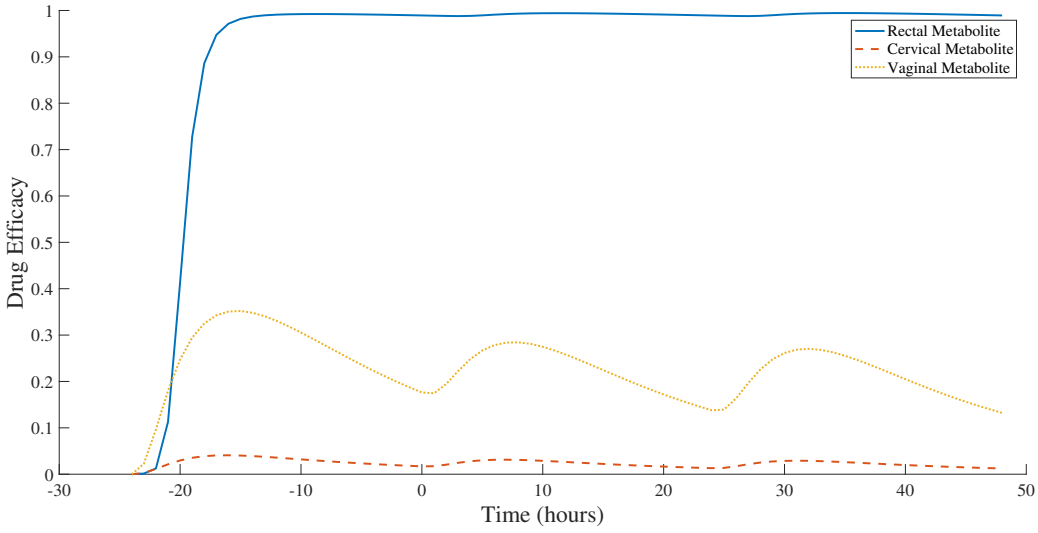

Figure 4.3: **Drug Efficacy of Time-Dependent Therapy.** We show how drug efficacy varies over time in the rectal, vaginal, and cervical metabolites, respectively, for a combined treatment of 400 mg of FTC and 600 mg of TDF 24 hours before exposure and 200 mg of FTC and 300 mg of TDF at and 24 hours after exposure to HIV. Model parameters are shown in Tables 4.1 and 4.2

In order to determine an effective dosing strategy, we vary the timing of the first dose from 24 hours before to at the time of exposure, the second dose from 0 to 24 hours following exposure, and the third dose from 24 to 48 hours after exposure and see how this affects the percent increase in the probability of extinction. We recall that our baseline probability of extinction was 99.66% without tratment. The following figures summarize our results.

In figure 4.4, we fix the time of Dose 1 to be 24 hours before exposure and vary the timing of Doses 2 and 3. In this case the maximum probability of extinction approaches is 99.98% when Doses 2 and 3 are administered 0 to 4 hours and 24 to 30 hours after exposure, respectively.

In figure 4.5, we fix the time of Dose 1 to be 13 hours before exposure and again vary the timing of Doses 2 and 3. We find that the maximum probability of extinction approaches 99.92% when Doses 2 and 3 are administered 0 to 2 hours and 24 to 35 hours after exposure, respectively.

In figure 4.6, we fix the time of Dose 1 to be 2 hours before exposure and again vary the timing of Doses 2 and 3. We find that the maximum probability of extinction approaches 99.90% when Doses 2 and 3 are administered at the time of exposure and either 24 hours or 27 to 38 hours after exposure, respectively.

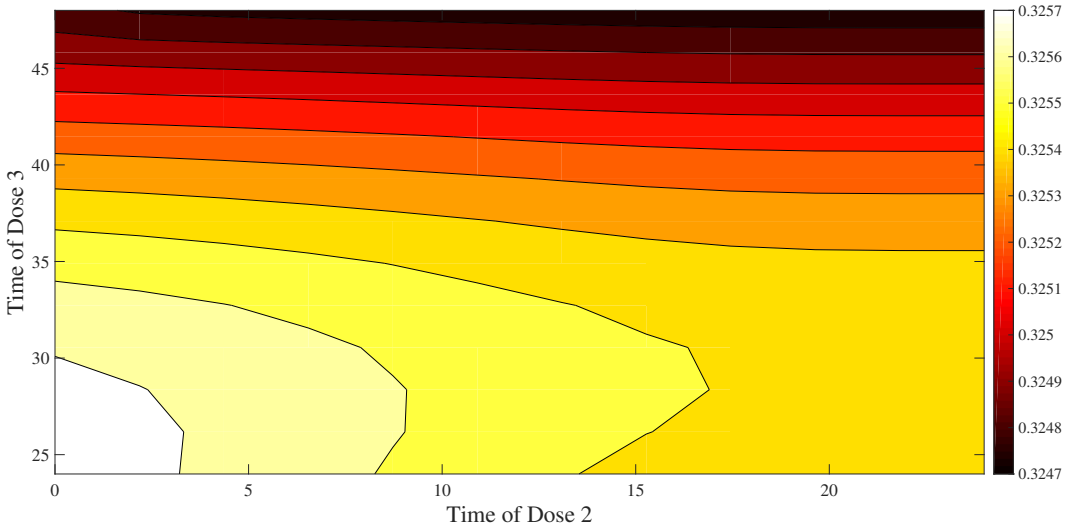

Figure 4.4: **Percent Increase in Probability of Extinction based on Time of Doses 2 and 3 if Dose 1 is Administered 24 Hours Before Exposure.** Colors and contours indicate the percentage increase in probability of extinction based on a varied dosing schedule. Dose 1 consists of 400 mg FTC and 600 mg TDF, while Doses 2 and 3 both consist of 200 mg FTC and 300 mg TDF. Parameters can be found in Table 2.2.

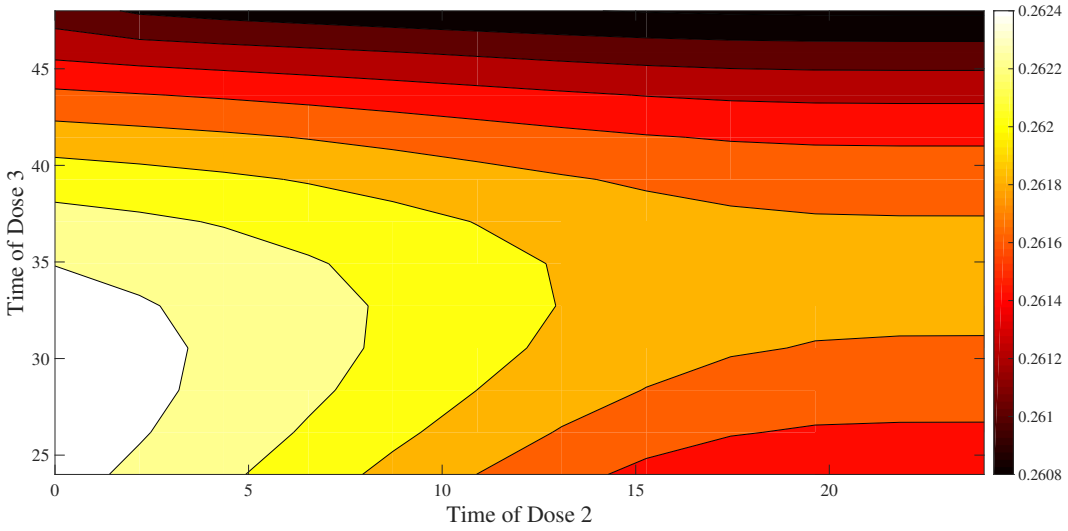

Figure 4.5: **Percent Increase in Probability of Extinction based on Time of Doses 2 and 3 if Dose 1 is Administered 13 Hours Before Exposure.** Colors and contours indicate the percentage increase in probability of extinction based on a varied dosing schedule. Dose 1 consists of 400 mg FTC and 600 mg TDF, while Doses 2 and 3 both consist of 200 mg FTC and 300 mg TDF. Parameters can be found in Table 2.2.

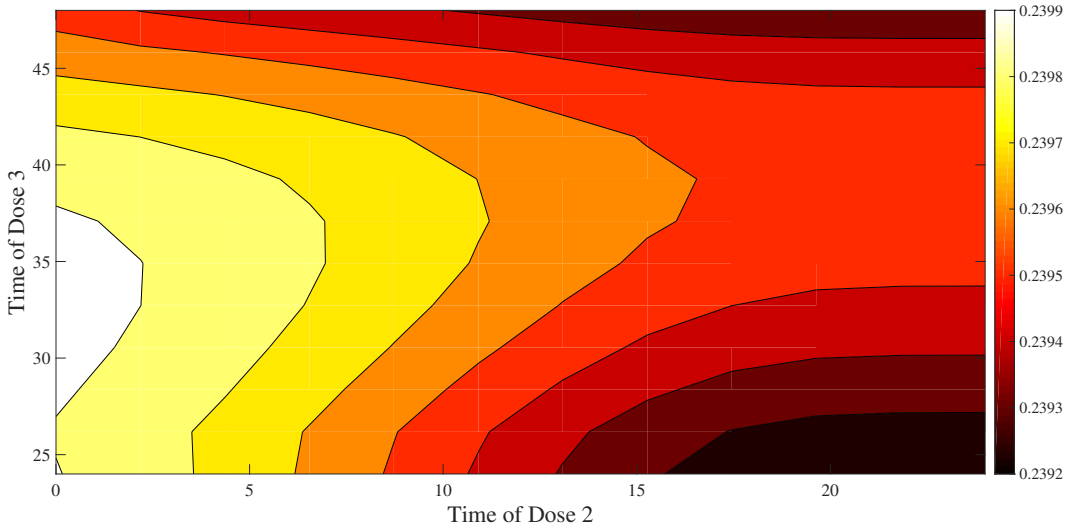

Figure 4.6: **Percent Increase in Probability of Extinction based on Time of Doses 2 and 3 if Dose 1 is Administered 2 Hours Before Exposure.** Colors and contours indicate the percentage increase in probability of extinction based on a varied dosing schedule. Dose 1 consists of 400 mg FTC and 600 mg TDF, while Doses 2 and 3 both consist of 200 mg FTC and 300 mg TDF. Parameters can be found in Table 2.2.

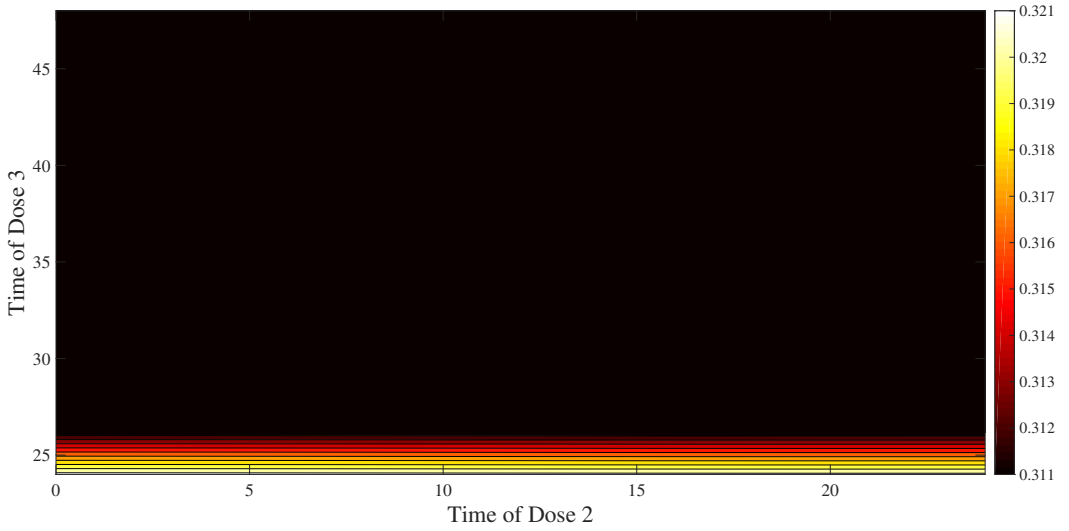

Figure 4.7: **Percent Increase in Probability of Extinction based on Time of Doses 2 and 3 if Dose 1 is Administered at the Time of Exposure.** Colors and contours indicate the percentage increase in probability of extinction based on a varied dosing schedule. Dose 1 consists of 400 mg FTC and 600 mg TDF, while Doses 2 and 3 both consist of 200 mg FTC and 300 mg TDF. Parameters can be found in Table 2.2.

In Figure 4.7, we fix the time of Dose 1 to be at the time of exposure and repeat the same process. We find that the maximum probability of extinction approaches 99.98% when Doses 2 and 3 are administered between 0 to 24 and at 24 hours after exposure, respectively.

From Figures 4.4-4.6, we show that the earlier before exposure that the first dose is administered, the greater the maximum probability of extinction is predicted. We also note that as the initial dose is taken closer to exposure time, Dose 2 must be administered earlier, and Dose 3 must be administered later. Figure 4.7 violates this trend, because the maximum probability of extinction approached when the first dose is taken at the time of exposure is the same as when it is taken 24 hours beforehand. However, this could very well be because of the high volume of drug being ingested within a small period of time. Practically speaking, such a large volume should be avoided if possible. Thus, our model predicts that for a maximum possible probability of extinction to be reached, the optimal dosing schedule is Dose 1 24 hours before exposure, Dose 2 0 to 4 hours after exposure, and Dose 3 24 to 30 hours after exposure. This is very similar to the dosing schedule used in the IPERGAY study of Dose 1 within 24 hours before exposure, Dose 2 at the time of exposure, and Dose 3 24 hours thereafter [2].

4.4 Conclusion

We successfully used a PK/PD model of the dynamics of Truvada to track how the drug travels throughout the body and used this information to calculate a time dependent drug efficacy based on the concentration of Truvada in the rectal metabolite over time. We then integrated this information into our original model of early HIV infection to provide recommendations for effective dosing schedules. Our final suggestion mimics the dosing schedule used by the IPERGAY study [2].

Chapter 5

Discussion

5.1 Discussion

Anti-retroviral therapy for HIV taken in advance of exposure to prevent infection, termed pre-exposure prophylaxis (PrEP), has been shown to decrease the risk of HIV [8] [9] [10]. However, some questions remain about the most efficient PrEP strategy. The CDC recommends daily dosing, taken for at least a month prior to exposure [1], but the IPERGAY study found that the risk of infection can be effectively controlled using short-term treatment administered only in the case of exposure. We investigated different PrEP strategies using a fully stochastic model of HIV. We focused on a single tissue model that considered the dynamics of four compartments: productively infected cells I_1, productively incompetent cells in the eclipse phase I_2, virus V, and incompetent virus W. We described our dynamics using a continuous time branching process and derived equations for probability generating functions (PGFs) using backwards Champman-Kolmogorov differential equations. We used the PGFs to predict the probability of infection prevention as the probability of extinction after exposure to one HIV viron. Typically, viral dynamics are studied using ordinary differential equations. However, differential equations describe average system behavior, and are therefore inappropriate for the study of early infection when viral and infected cell populations are small. Further, our emphasis is the probability of infection clearance, which cannot be described using ODEs. Thus, our approach is the use of stochastic, Markov chain models. These are frequently studied via simulation [3], but in the interest of efficiency, we instead use a mathematical approach that avoids calling on extensive and time-intensive simulation.

We first investigated PrEP assuming constant drug efficacy, predicting that PrEP effectively prevents HIV infection. We found that for a fixed efficacy, RTIs provide greater protection than PIs and that the impact of RTIs is observed much faster, suggesting that if PrEP is interrupted shortly after exposure, RTIs are more effective. This suggests that long-term therapy after exposure may be unnecessary and that short-term therapy could provide the same level of protection. However, the duration of therapy remains unclear.

To study which dosing schedules are effective, we needed a pharmacokinetic-pharmacodynamic

model of Truvada, the FDA-approved drug used in PrEP. Realistically, drug distribution in the body exhibits time-dependent behavior. We used a PK/PD compartmental model proposed by Cottrell et. al of how the RTIs which make up Truvada, tenofovir disoproxil fumerate (TDF) and emtricitabine (FTC), travel through the body to calculate a time-dependent drug efficacy [4]. We then integrated the PK/PD model into our original model of early HIV dynamics to find the best treatment strategy for PrEP.

Our model predicts that in order to achieve the greatest percent increase in the probability of extinction, two pills of Truvada should be taken 24 hours before exposure, one pill should be taken 0 to 4 hours following exposure, and one pill should be taken 24 to 30 hours after exposure. This suggests that "on-demand" pre exposure prophylaxis can be a viable option for HIV prevention. This schedule of dosing is very similar to that used by the highly successful IPERGAY clinical trial, which used a schedule of two pills within 24 hours of exposure and one pill at 24 hours and 48 hours following exposure. [2]. Note that in the present study, we focused on the primary mode of transmission for men who have sex with men (MSM), the focus of the IPERGAY study. We leave efficacy of on-demand PrEP for women for future study, but recognize that drug absorption into cervical and vaginal tissues is slower than rectal tissue, so we anticipate our predictions will suggest on-demand PrEP to be less effective for women.

Naturally, our model has some limitations. We initiate infection with a single, infectious virus. Viral innocula are much larger, although much of that is not infectious. We note that our predictions showed only modest enhancements in p_extt with different drug regimens. We anticipate these enhancements will be larger with a more realistic inoculum, since baseline risk of infection is higher. However, we do not expect our qualitative predictions to change. In future work, we will consider a mix of infectious and non-infectious virus [11]. All in all, we anticipate our qualitative and relative results will remain the same. Similarly, our PK/PD model predicted drug absorption in tissues to be more rapid than that observed in other studies [23] [24]. Fortunately, this does not affect our qualitative results with respect to best times of dosing, but this does affect our quantitative results with respect to the actual percent increase in the probability of extinction. Finally, our

model captures only the dynamics in a single tissue compartment. Experimental evidence suggests that different cell types and transport between the periphery and various bodily tissues contribute to the initiation of HIV infection [25]. This suggests that an improved model would have at least two additional compartments, such as the lymph in addition to rectal tissues.

Overall, we presented new theoretical predictions on the early dynamics of HIV infection including the pharmacokinetics/pharmacodynamics of PrEP that are difficult to obtain experimentally. Our results support the use of "on demand" pre-exposure prophylaxis and suggest more narrow guidelines for improved protection from HIV. An improved model of HIV infection and improved parameter estimates for our pharmacokinetic model would allow us to further improve our treatment recommendations. We believe that models like those presented in this paper can continue to be used to improve our understanding of HIV prevention and treatment.

Chapter 6

Appendix

6.1 Chapter 2 Code

```
%%This script runs a simulation for whether exposure to one
%%viron leads to extinction or persistent infection.

for k = 1:12
clear
%%%%%Parameters
V(1)= 1; %viron
I(1)=0; %infected
t(1)=0; %time
N = 10; %innoculum size
kT=10;
d=1;
c=20;

%%%%% Initial Value
j = 1;

while (I(j)+V(j)>0)&&(I(j)<=32) %While there are still infected cells
   and virons and infected cells are below detection threshold
   j = j+1; %%% rates of states
   a1= kT*V(j-1);
   a2= N*d*I(j-1);
   a3=d*I(j-1);
   a4=c*V(j-1);
   a0= a1+a2+a3+a4;
```

```
    r1=rand;

    tau = ((1/a0) * log(1/r1)); %%time step

    t(j)= t(j-1) + tau;

    r2= rand(1); %%%random probability

    if r2 <= a1/a0 %%probability of the reactionis the rate of the
       state over the sum of all the rates of states
       I(j) = I(j-1)+1;
       V(j) = V(j-1) -1;
    elseif (a1/a0 < r2)&&(r2<= (a2+a1)/a0)
       I(j) = I(j-1);
       V(j) = V(j-1) +1;
    elseif ((a1+a2)/a0 <r2)&&(r2<=(a1+a2+a3)/a0)
       I(j) = I(j-1) -1;
       V(j) = V(j-1);
    else
       I(j) = I(j-1);
       V(j) = V(j-1)-1;
    end
end


figure(1)
subplot(1,2,1)
set(gca, 'Fontsize', 18)
hold on
```

```
plot(t, I, 'linewidth', 2)
xlabel('Time (days)','FontSize', 18)
ylabel('Number of Infected Cells', 'Fontsize', 18)

subplot(1,2,2)
hold on
set(gca, 'Fontsize', 18)
plot(t, V, 'linewidth', 2)
xlabel('Time (days)','FontSize', 18)
ylabel('Number of Virus','FontSize', 18)
end
```

6.2 Chapter 3 Code

```
clear all

%This script generates all plots for Constant Efficacy PrEP

%% Percent Increase in Probability of Extinction varying drug Efficacy
epsM=0:.01:1; %RTI drug Efficacy
epsMM=0:.01:1; %PI drug Efficacy

for jj=1:length(epsM)
   [pextI,pextV, pext_Vis1]=HIVTimeDiff3(epsM(jj),0, 2);
   C(jj) = pextV
   C(jj)=((pextV-pext_Vis1)/pext_Vis1) * 100;
end
```

```
for kk=1:length(epsMM)
   [pextI1,pextV1, pext_Vis11]=HIVTimeDiff3(0,epsMM(kk), 2);
   D(kk) = pextV1
   D(kk)=((pextV1-pext_Vis11)/pext_Vis11) * 100;
end

maxprobRTI = (C(end)/100)*(pext_Vis1) + (pext_Vis1);
maxprobPI = (D(end)/100)*(pext_Vis1) + (pext_Vis1);

figure (1)
hold on
plot(epsM, C, 'linewidth', 2)
plot(epsMM, D, 'linewidth', 2')
xlabel('Drug Efficacy', 'FontName', 'Times', 'Fontsize', 24)
ylabel('Percent Increase in Probability of Extinction', 'FontName',
   'Times', 'Fontsize', 24)
legend('RTI', 'PI')


%% Percent Increase in Prob. of Extinction vs stop time
tend=0:.1:24;
for jj=1:length(tend)
   [pextI,pextV, pext_Vis1]=HIVTimeDiff3(0.8,0,tend(jj));
   A(jj)=(pextV-pext_Vis1)/pext_Vis1 * 100;
   N(jj) = pextV;
end

for kk=1:length(tend)
   [pextI,pextV, pext_Vis1]=HIVTimeDiff3(0,0.8,tend(kk));
```

```
    B(kk)=(pextV-pext_Vis1)/pext_Vis1 * 100;
    M(kk) = pextV;
end

maxprobRTI = (A(end)/100)*pext_Vis1 + pext_Vis1;
maxprobPI = (B(end)/100)*pext_Vis1 + pext_Vis1;

figure (2)
hold on
plot(tend, A, 'linewidth', 2)
plot(tend, B, 'linewidth', 2)
xlabel('Duration of Treatment')
ylabel('Percent Increase in Probability of Extinction') %or would
    probability of extinction suffice?
legend('RTI', 'PI')
%
N = 10;
kT=10;
d=1;
c=20;
eps=0.8;
pextV_inf=min(1-((N*kT*(1-eps))/(c+kT*(1-eps))-1)/N,1)

%% contour plot of Percent risk of Infection varying efficacy and tend

epsM=0:.01:1;
tend=0:.1:12;
B = zeros(length(epsM), length(tend));
```

```
%to generate PI graph
for ll=1:length(epsM)
   ll
   for kk=1:length(tend)
      [pextI,pextV, pext_Vis1]=HIVTimeDiff3(0,epsM(ll), tend(kk));
      B(ll,kk)=((pextV-pext_Vis1)/pext_Vis1) * 100 ;
   end
end

% to generate RTI graph

% for ll=1:length(epsM)
%    ll
%    for kk=1:length(tend)
%       [pextI,pextV, pext_Vis1]=HIVTimeDiff3(epsM(ll),0, tend(kk));
%       B(ll,kk)=((pextV-pext_Vis1)/pext_Vis1) * 100 ;
%    end
% end

figure(4)
contourf(epsM,tend,B')
colorbar
%caxis([0.75,1]);
colormap jet
%l1 = line([0.6,0.6],[0,3]);
%set(l1,'Linewidth',3,'Color',[1,1,1],'Linestyle','--')
xlabel('Drug Efficacy')
ylabel('Time of PreP Interruption Relative to HIV Exposure')
```

```
%% contour plot combo therapy
epsM=0:.01:1; %RTI
epsMM = 0:.01:1; %PI
B = zeros(length(epsM), length(epsMM));
for ll=1:length(epsM)
   ll
   for kk=1:length(epsMM)
      [pextI,pextV, pext_Vis1]=HIVTimeDiff3(epsM(ll) ,epsMM(kk),10);
      B(ll,kk)=((pextV-pext_Vis1)/pext_Vis1) * 100 ;
   end
end

figure(4)
contourf(epsM,epsMM,B')
colorbar
colormap jet
xlabel('Drug Efficacy RTI')
ylabel('Drug Efficacy PI')
```

```
function [pextI,pextV, pext_Vis1]=HIVTimeDiff3(epsM, epsMM, tend)
%Solves equations backwards in Time to obtain probabilities of
   extinction

%PreP

%Parameters

N = 5000;
d=1;
```

```
c=23;
R0 = 2.70;
s = 1;
Q = .1;
kT = c*R0/(N*Q-R0);

pars = [N;R0;d;c;epsM;epsMM;tend;Q;s;kT];

options = odeset('RelTol', 1e-12, 'AbsTol', 1e-12);

[T,Y] = ode45(@(t,y)kin2(pars,t,y), [100:-1:0], [0;0;0], options);

pextI=Y(end,1);
pextV=Y(end,2);

%pext_Iis1 = (c+kT*(1-eps))/(N*kT*(1-eps)); % 1/R0
pext_Vis1 = min(1, 1-(R0-1)/(N*Q));
% pext = pext_Iis1^0*pext_Vis1^1;

% plot(T(2:end),diff(Y(:,1).^0.*Y(:,2).^1)/.01/pext,'r','Linewidth',2)

end
```

```
function dy=kin2(pars,t,y)
%differential equation system for more detailed model

%Parameters
N = pars(1);
R0= pars(2);
```

```
d = pars(3);

c = pars(4);

epsM = pars(5);

epsMM = pars(6);

tend = pars(7);

Q = pars(8);

s = pars(9);

kT = pars(10);


epsRTI = 0;

epsPI = 0;

if t<=tend

   epsRTI = epsM;

   epsPI = epsMM;

else

   epsRTI=0;

   epsPI = 0;

end



dy(1,1) = -d*(1-y(1))-(1-epsPI)*Q*N*d*y(1)*(y(2)-1);


dy(2,1) = -c*(1-y(2)) - (1 - epsRTI)*kT*(y(3)-y(2));


dy(3,1) = -s*(y(1)-y(3));


end
```

6.3 Chapter 4 Code

```
function [T,Z] = DrugPlot(option, graph, tdose)
%%%%% Solves system of diff. eqs for PK/PD model and provides plots of
%%%%% dynamics in every compartment

options = odeset('RelTol', 1e-12, 'AbsTol', 1e-12);

if option == 1
% parameters for FTC
D0 = .2; %100, 200
Kg = 1;
Kgr = .033;
Ka = .649;
Vc= 72.3;
Vp = 122;
Q = 6.06;
CLtt = 18.9;
Fv = .00131;
Fe = .000069;
Fr = .00401;
Fvt = .325;
CLttvvtp = .0101;
CLvvtp = .0399;
Fet = 1;
CLttve = .000947;
Fet = 1;
CLttve = .000947;
```

```
CLvetp = .0082;

Frt = .0107;

CLttvr = .0223;

CLvrtp = .647;

Kt = .0724;

Kga = 1;


else


%Parameters for TFV

D0 = .3; %150, 300

Kg = 1;

Kgr = .033;

Ka = .863;

Vc = 331;

Vp = 843;

Q = 142;

CLtt = 58.7;

Fv = .000079;

Fe = .000015;

Fr= .00007;

Fvt = .243;

CLttvvtp = .0111;

CLvvtp = .041;

Fet = .0292;

CLttve = .00183;

CLvetp = .00207;

Frt = .1;

CLttvr = .00477;
```

```
CLvrtp = .14;
Kt = .0752;
Kga = .0589;
end

pars = [Kg,Kgr,Ka,Vc,Vp,Q,CLtt,Fv,Fe,Fr,Fvt,CLttvvtp,CLvvtp,Fet,CLttve,
   Fet,CLttve,CLvetp,Frt,CLttvr,CLvrtp,Kt,Kga,D0];

 %[T,Z] = ode45(@(t,z)drugdynamics2(tdose,t,z), [0:.1:100],
    [0;0;0;0;0;0;0;0;0;0;0;0;0;0;0], options);
[T,Z] = ode45(@(t,z)drugdynamics2(pars,tdose,t,z), [-24:1:48],
   zeros(1,15), options);
%%
%
% figure(1)
% %plot(T(end-100:end), log(Z(end-100:end,1)*1e6/1e3))
% subplot(3,2,1);
% plot(T, log(Z(:,1)),'Linewidth',3)
% xlabel('Time (hours)')
% ylabel('log Drug Concentration Gut1') %%%%add log to all y labels
%
% subplot(3,2,2);
% plot(T, log(Z(:,2)),'Linewidth',3)
% xlabel('Time (hours)')
% ylabel('Drug Concentration Gut2')
%
% subplot(3,2,3);
% plot(T, log(Z(:,3)),'Linewidth',3)
% xlabel('Time (hours)')
```

```
% ylabel('Drug Concentration Gut3')
%
% subplot(3,2,4);
% plot(T, log(Z(:,4)),'Linewidth',3)
% xlabel('Time (hours)')
% ylabel('Drug Concentration Gut4')
%
% subplot(3,2,5);
% plot(T, log(Z(:,5)),'Linewidth',3)
% xlabel('Time (hours)')
% ylabel('Drug Concentration Gut5')
%
% subplot(3,2,6);
% plot(T, log(Z(:,6)),'Linewidth',3)
% xlabel('Time (hours)')
% ylabel('Drug Concentration Gut6')
%
% figure(2)
%
% subplot(3,3,1);
% plot(T, log(Z(:,7)),'Linewidth',3)
% xlabel('Time (hours)')
% ylabel('Drug Concentration Gut7')
%
% subplot(3,3,2);
% plot(T, log(Z(:,8)),'Linewidth',3)
% xlabel('Time (hours)')
% ylabel('Drug Concentration Rectal')
%
```

```
% subplot(3,3,3);
% plot(T, log(Z(:,9)),'Linewidth',3)
% xlabel('Time (hours)')
% ylabel('Drug Concentration RecMet')
%
% subplot(3,3,4);
% plot(T, log(Z(:,10)),'Linewidth',3)
% xlabel('Time (hours)')
% ylabel('Drug Concentration Distribution')
%
% subplot(3,3,5);
% plot(T, log(Z(:,11)),'Linewidth',3)
% xlabel('Time (hours)')
% ylabel('Drug Concentration Plasma')
%
% subplot(3,3,6);
% plot(T, log(Z(:,12)),'Linewidth',3)
% xlabel('Time (hours)')
% ylabel('Drug Concentration Cervical')
% %%%%%%%%%%%%%%%%%%%%%%
% figure(3)
% subplot(3,1,1);
% plot(T, log(Z(:,13)),'Linewidth',3)
% xlabel('Time (hours)')
% ylabel('Drug Concentration Cervical Met')
%
% subplot(3,1,2);
% plot(T, log(Z(:,14)),'Linewidth',3)
% xlabel('Time (hours)')
```

```
% ylabel('Drug Concentration Vaginal')
%
% subplot(3,1,3);
% plot(T, log(Z(:,15)),'Linewidth',3)
% xlabel('Time (hours)')
% ylabel('Drug Concentration Vaginal Met')

% figure(4)
% semilogy(T,Z(:,10),'Linewidth',3)
% xlabel('Time (hours)')
% ylabel('Drug Concentration Distribution')

%% WITHOUT LOGS
%
if graph== 1
    figure(1)
    %plot(T(end-100:end), log(Z(end-100:end,1)*1e6/1e3))
    subplot(3,2,1);
    plot(T, (Z(:,1)),'Linewidth',3)
    xlabel('Time (hours)')
    ylabel('Drug Concentration Gut1') %%%%add log to all y labels

    subplot(3,2,2);
    plot(T, (Z(:,2)),'Linewidth',3)
    xlabel('Time (hours)')
    ylabel('Drug Concentration Gut2')

    subplot(3,2,3);
    plot(T, (Z(:,3)),'Linewidth',3)
```

```
xlabel('Time (hours)')
ylabel('Drug Concentration Gut3')

subplot(3,2,4);
plot(T, (Z(:,4)),'Linewidth',3)
xlabel('Time (hours)')
ylabel('Drug Concentration Gut4')

subplot(3,2,5);
plot(T, (Z(:,5)),'Linewidth',3)
xlabel('Time (hours)')
ylabel('Drug Concentration Gut5')

subplot(3,2,6);
plot(T, (Z(:,6)),'Linewidth',3)
xlabel('Time (hours)')
ylabel('Drug Concentration Gut6')

figure(2)

subplot(3,3,1);
plot(T, (Z(:,7)),'Linewidth',3)
xlabel('Time (hours)')
ylabel('Drug Concentration Gut7')

subplot(3,3,2);
plot(T, (Z(:,8)),'Linewidth',3)
xlabel('Time (hours)')
ylabel('Drug Concentration Rectal')
```

```
subplot(3,3,3);
plot(T, (Z(:,9)),'Linewidth',3)
xlabel('Time (hours)')
ylabel('Drug Concentration Rectal Metabolite')

subplot(3,3,4);
plot(T, (Z(:,10)),'Linewidth',3)
xlabel('Time (hours)')
ylabel('Drug Concentration Distribution')

subplot(3,3,5);
plot(T, (Z(:,11)),'Linewidth',3)
xlabel('Time (hours)')
ylabel('Drug Concentration Plasma')

subplot(3,3,6);
plot(T, (Z(:,12)),'Linewidth',3)
xlabel('Time (hours)')
ylabel('Drug Concentration Cervical')
%%%%%%%%%%%%%%%%%%%%%%%%
figure(3)
subplot(3,1,1);
plot(T, (Z(:,13)),'Linewidth',3)
xlabel('Time (hours)')
ylabel('Drug Concentration Cervical Metabolite')

subplot(3,1,2);
plot(T, (Z(:,14)),'Linewidth',3)
```

```
    xlabel('Time (hours)')
    ylabel('Drug Concentration Vaginal')

    subplot(3,1,3);
    plot(T, (Z(:,15)),'Linewidth',3)
    xlabel('Time (hours)')
    ylabel('Drug Concentration Vaginal Metabolite')

    figure(4)
    hold on
    plot(T, (Z(:,13)),'Linewidth',3)
    plot(T, (Z(:,9)),'Linewidth',3)
    plot(T, (Z(:,15)),'Linewidth',3)
    xlabel('Time (hours)', 'FontSize', 24)
    ylabel('Concentration of FTC', 'FontSize', 24)
    legend('Cervical Metabolite', 'Rectal Metabolite', 'Vaginal
       Metabolite')
%
%    figure(5)
%    plot(T, (Z(:,9)),'Linewidth',3)
%    xlabel('Time (hours)', 'FontSize', 24)
%    ylabel('Concentration of FTC in Rectal Metabolite','FontSize', 24)
%
%    figure(6)
%    plot(T, (Z(:,15)),'Linewidth',3)
%    xlabel('Time (hours)', 'FontSize', 24)
%    ylabel('Concentration of FTC Vaginal Metabolite','FontSize', 24)
%
%
```

```
end


end
```

```
function dz = drugdynamics2(pars,tdose,t,z)
%Differential equations for PK/PD Model

%Parameters
Kg = pars(1);
Kgr = pars(2);
Ka = pars(3);
Vc= pars(4);
Vp = pars(5);
Q = pars(6);
CLtt = pars(7);
Fv = pars(8);
Fe = pars(9);
Fr = pars(10);
Fvt = pars(11);
CLttvvtp = pars(12);
CLvvtp = pars(13);
Fet = pars(14);
CLttve = pars(15);
Fet = pars(16);
CLttve = pars(17);
CLvetp = pars(18);
Frt = pars(19);
CLttvr = pars(20);
CLvrtp = pars(21);
```

```
Kt = pars(22); %%%%%%%%
Kga = pars(23);
D0 = pars(24);


%Dependent Variables
G1 = z(1,1);
G2 = z(2,1);
G3 = z(3,1);
G4 = z(4,1);
G5 = z(5,1);
G6 = z(6,1);
G7 = z(7,1);
Rec = z(8,1);
RecMet = z(9,1);
Dist = z(10,1);
P = z(11,1);
Cerv = z(12,1);
CervMet = z(13,1);
Vaginal = z(14,1);
VaginalMet = z(15,1);

D = D0 * (Kg + Ka) * sum(exp(-(Kg+Ka)*(t-tdose)).*heaviside(t-tdose));

%Gut
dz(1,1) = Kg*(D-G1);
dz(2,1) = Kg*(G1-G2);
dz(3,1) = Kg*(G2-G3);
dz(4,1) = Kg*(G3-G4);
```

```
dz(5,1) = Kg*(G4-G5);
dz(6,1)= Kg*(G5-G6);
dz(7,1) = Kg*G6 - Kgr*G7 - Kga * G7;

%Rectal
dz(8,1) = Kga* G7 + Fr*CLtt*P/Vc - CLttvr * Rec/.17;
dz(9,1) = Frt*CLttvr*Rec/.17 - CLvrtp* RecMet/.17;

%Distribution
dz(10,1) = P*Q/Vc -Dist * Q/Vp;

%Plasma
dz(11,1) = Ka * D -Q*P/Vc+ Dist*Q/Vp - CLtt*P/Vc; %%%Check this

%Cervical
dz(12,1) = Fe*CLtt * P/Vc - CLttve*Cerv/.01;
dz(13,1) = Fet*CLttve*Cerv/.01 - CLvetp*CervMet/.01;

%Vaginal
dz(14,1) = Fv*CLtt*P/Vc - CLttvvtp * Vaginal/.09;
dz(15,1) = Fvt*CLttvvtp*Vaginal/.09 - CLvvtp * VaginalMet/.09;
end
```

```
function [pextI,pextV, pext_Vis1]=HIVTimeDiff3(epsM, epsMM, tend)
%Solves equations backwards in Time to obtain probabilities of
   extinction

%PreP
```

```
%Parameters

N = 5000;
d=1;
c=23;
R0 = 2.70;
s = 1;
Q = .1;
kT = c*R0/(N*Q-R0);

pars = [N;R0;d;c;epsM;epsMM;tend;Q;s;kT];

options = odeset('RelTol', 1e-12, 'AbsTol', 1e-12);

[T,Y] = ode45(@(t,y)kin2(pars,t,y), [100:-1:0], [0;0;0], options);

pextI=Y(end,1);
pextV=Y(end,2);

%pext_Iis1 = (c+kT*(1-eps))/(N*kT*(1-eps)); % 1/R0
pext_Vis1 = min(1, 1-(R0-1)/(N*Q));
% pext = pext_Iis1^0*pext_Vis1^1;

% plot(T(2:end),diff(Y(:,1).^0.*Y(:,2).^1)/.01/pext,'r','Linewidth',2)

end
```

```
%%Calculate Efficacy for various dose times
%tdose = [i,j,k] and loop through different values for i, j, and k
```

```
clear all
%
linspace(-24,0,12);
tdose2 = linspace(0,24,12);
tdose3 = linspace(24,48,12);
B = zeros(length(tdose2), length(tdose3));

for k = 1:length(tdose1)
for i = 1:length(tdose2)
   for j = 1:length(tdose3)
      eps=Efficacy([tdose1(k), tdose1(k), tdose2(i), tdose3(j)]);
      [pextI,pextV]= HIVTimeDiffChangingEfficacy(eps);
      B(k,i,j) = pextV
   end
end
end

MAT1 = squeeze(B(1,:,:));
MAT2 = squeeze(B(6,:,:));
MAT3 = squeeze(B(11,:,:));
MAT4 = squeeze(B(12,:,:));

%Dose 1 at -24 hours
figure(1)
contourf(tdose2, tdose3,((MAT1-.9966)./.9966) * 100);
colorbar
colormap heat
xlabel('Time of Dose 1 (hours)')
ylabel('Time of Dose 2 (hours)')
```

```
%Dose 1 at -13 hours
figure(2)
contourf(tdose2, tdose3,((MAT2-.9966)./.9966) * 100);
colorbar
colormap heat
xlabel('Time of Dose 1 (hours)')
ylabel('Time of Dose 2 (hours)')

%Dose 1 at -2 hours
figure(3)
contourf(tdose2, tdose3,((MAT4-.9966)./.9966) * 100);
colorbar
colormap heat
xlabel('Time of Dose 1 (hours)')
ylabel('Time of Dose 2 (hours)')

%Dose 1 at exposure
figure(3)
contourf(tdose2, tdose3,((MAT4-.9966)./.9966) * 100);
colorbar
colormap heat
xlabel('Time of Dose 1 (hours)')
ylabel('Time of Dose 2 (hours)')
```

```
function [pextI,pextV,T,Y]=HIVTimeDiffChangingEfficacy(eps)

%Solves diff. eqs backwards in time for system with changing drug
   efficacy
```

```
%PreP

%Params

N = 5000;
R0 = 2.70;
d=1;
c=23;
Q = .1;
s = 1;

pars = [N; R0; d; c; Q; s];

options = odeset('RelTol', 1e-12, 'AbsTol', 1e-12);

I = find(eps(:,2)>0,1);
tfirstdose = eps(I,1);

[T,Y] = ode45(@(t,y)changingefficacy(pars, eps ,t, y),
   [eps(end,1),tfirstdose]/24, [0; 0; 0], options);

pextI = Y(end,1);
pextV=Y(end,2);



end
```

```
function dy=changingefficacy(pars, eps ,t,y)

%diff. eqs for more detailed early infection HIV model coupled with
   time
%dependent efficacy

N = pars(1);
R0= pars(2);
d = pars(3);
c = pars(4);
Q = pars(5);
s = pars(6);

kT = c*R0/(N*Q-R0);

epsRTI = interp1(eps(:,1)/24,eps(:,2),t,'linear');

dy(1,1) = -d*(1-y(1))-Q*N*d*y(1)*(y(2)-1);

dy(2,1) = -c*(1-y(2)) - (1 - epsRTI)*kT*(y(3)-y(2));

dy(3,1) = -s*(y(1)-y(3));

end
```

Bibliography

[1] Center for Disease Control and Prevention. US Public Health Service. Preexposure Prophylaxis for the Prevention of Infection in the United States-2014. Report, Center for Disease Control and Prevention, 2014.

[2] Jean-Michel Molina. IPERGAY. Report, Global Advocacy for HIV Prevention, 2016.

[3] John E. Pearson, Paul Krapivsky, and Alan S. Perelson. Stochastic Theory of Early Viral Infection: Continuous versus Burst Production of Virions. *PLOS Computational Biology*, 7(2), FEB 2011.

[4] Mackenzie L Cottrell, Kuo H Yang, Heather MA Prince, Craig Sykes, Nicole White, Stephanie Malone, Evan S Dellon, Ryan D Madanick, Nicholas J Shaheen, Michael G Hudgens, et al. A Translational Pharmacology Approach to Predicting Outcomes of Preexposure Prophylaxis against HIV in Men and Women Using tenofovir disoproxil fumarate with or without emtricitabine. *The Journal of Infectious Diseases*, 214(1):55–64, 2016.

[5] Martin A. Nowak and Robert M. May. *Virus Dynamics: Mathematical Principles of Immunology and Virology*. Oxford Unversity Press, 2004.

[6] Denise M Cardo, David H Culver, Carol A Ciesielski, Pamela U Srivastava, Ruthanne Marcus, Dominique Abiteboul, Julia Heptonstall, Giuseppe Ippolito, Florence Lot, Penny S McKibben, et al. A Case–Control Study of HIV Seroconversion in Health Care Workers after Percutaneous Exposure. *New England Journal of Medicine*, 337(21):1485–1490, 1997.

[7] Center for Disease Control and Prevention. Updated Guidelines for Antiretroviral Postexposure Prophylaxis After Sexual, Injection Drug Use, or Other Nonoccupational Exposure to HIV United States, 2016. Report, Center for Disease Control and Prevention, 2016.

[8] Lisa A Grohskopf, Kata L Chillag, Roman Gvetadze, Albert Y Liu, Melanie Thompson, Kenneth H Mayer, Brandi M Collins, Sonal R Pathak, Brandon O'Hara, Marta L Ackers, et al. Randomized Trial of Clinical Safety of Daily Oral tenofovir disoproxil fumarate Among HIV-Uninfected Men who have Sex with Men in the United States. *JAIDS Journal of Acquired Immune Deficiency Syndromes*, 64(1):79–86, 2013.

[9] Jared M Baeten, Deborah Donnell, Patrick Ndase, Nelly R Mugo, James D Campbell, Jonathan Wangisi, Jordan W Tappero, Elizabeth A Bukusi, Craig R Cohen, Elly Katabira, et al. Antiretroviral Prophylaxis for HIV Prevention in Heterosexual Men and Women. *New England Journal of Medicine*, 367(5):399–410, 2012.

[10] Robert M Grant, Javier R Lama, Peter L Anderson, Vanessa McMahan, Albert Y Liu, Lorena Vargas, Pedro Goicochea, Martín Casapía, Juan Vicente Guanira-Carranza, Maria E Ramirez-Cardich, et al. Preexposure chemoprophylaxis for HIV prevention in Men who have Sex with Men. *New England Journal of Medicine*, 363(27):2587–2599, 2010.

[11] Jessica M. Conway, Bernhard P. Konrad, and Daniel Coombs. Stochastic Analysis of Pre- and Postexposure Prophylaxis against HIV Infection. *SIAM Journal of Applied Mathematics*, 73(2):904–928, 2013.

[12] Daniel T Gillespie. Exact Stochastic Simulation of Coupled Chemical Reactions. *The Journal of Physical Chemistry*, 81(25):2340–2361, 1977.

[13] S Karlin and HM Taylor. *A First Course in Stochastic Processes*. Academic Press, New York, 1975.

[14] Peter Rusert, Marek Fischer, Beda Joos, Christine Leemann, Herbert Kuster, Markus Flepp, Sebastian Bonhoeffer, Huldrych F Günthard, and Alexandra Trkola. Quantification of In-

fectious HIV-1 Plasma Viral Load Using a Boosted in vitro Infection Protocol. *Virology*, 326(1):113–129, 2004.

[15] Narendra M Dixit, Martin Markowitz, David D Ho, and Alan S Perelson. Estimates of Intracellular Delay and Average Drug Efficacy from Viral Load Data of HIV-infected Individuals Under Antiretroviral Therapy. *Antivir. Ther*, 9(2):237–246, 2004.

[16] Rob J. De Boer, Ruy M. Ribeiro, and Alan S. Perelson. Current Estimates for HIV-1 Production Imply Rapid Viral Clearance in Lymphoid Tissues. *PLOS Computational Biology*, 6(9), SEP 2010.

[17] Hannah Yuan Chen, Michele Di Mascio, Alan S. Perelson, David D. Ho, and Linqi Zhang. Determination of virus burst size in vivo using a single-cycle SIV in rhesus macaques. *Proceedings of the National Academy of Sciences of the United States of America*, 104(48):19079–19084, NOV 27 2007.

[18] A. Aldovini and R.A. Young. Mutations of RNA and Protein Sequences Involved in Human Immunodeficiency Virus Type 1 Packaging Result in Production of Noninfectious Virus. *J Virol*, 64:1920–1926, 1990.

[19] Ruy M. Ribeiro, Li Qin, Leslie L. Chavez, Dongfeng Li, Steven G. Self, and Alan S. Perelson. Estimation of the Initial Viral Growth Rate and Basic Reproductive Number during Acute HIV-1 Infection. *Journal of Virology*, 84(12):6096–6102, JUN 2010.

[20] Department of Health and Human Services. FDA-Approved HIV Medicines.

[21] Yves Pommier, Allison A Johnson, and Christophe Marchand. Integrase Inhibitors to Treat HIV/AIDS. *Nature Reviews Drug Discovery*, 4(3):236, 2005.

[22] S Jing, Qian Zhao, and Asim K Debnath. Peptide and Non-peptide HIV Fusion Inhibitors. *Current pharmaceutical design*, 8(8):563–580, 2002.

[23] Kristine B Patterson, Heather A Prince, Eric Kraft, Amanda J Jenkins, Nicholas J Shaheen, James F Rooney, Myron S Cohen, and Angela DM Kashuba. Penetration of tenofovir and emtricitabine in Mucosal Tissues: Implications for Prevention of HIV-1 Transmission. *Science translational medicine*, 3(112):112re4–112re4, 2011.

[24] Peter L Anderson, Jennifer J Kiser, Edward M Gardner, Joseph E Rower, Amie Meditz, and Robert M Grant. Pharmacological Considerations for tenofovir and emtricitabine to Prevent HIV Infection. *Journal of Antimicrobial Chemotherapy*, 66(2):240–250, 2010.

[25] AT Haase. Population Biology of HIV-1 Infection: Viral and CD4+ T Vell Demographics and Dynamics in Lymphatic Tissues. *Annual review of immunology*, 17(1):625–656, 1999.

Academic Vita

Olga Dorabiala

Education

Pennsylvania State University, University Park **2014-2018**

Schreyer Honors College

Eberly College of Science, Major in Applied and Industrial Mathematics

Eberly College of Science, Minor in Chemistry

College of the Liberal Arts, Minor in German

Pennsylvania State University, Altoona Campus **2013-2014**

Dual Enrollment

Calculus with Analytic Geometry II, Fall 2013; Calculus and Vector Analysis, Spring 2014

Research Experience

Undergraduate Research with Dr. Jessica Conway **2016-present**

Writing honors thesis on the spread of HIV infection. To be completed in Spring 2018.

Developing a mathematical model of early HIV infection based on virus dynamics and the pharmacokinetics of HIV drugs in order to better inform and providing testable predictions for HIV pre-exposure prophylaxis (PREP) treatments.

Deep Learning for Face Recognition **Fall 2017**

Working with a team of students to develop face recognition software that can perform with high accuracy on the large-scale MegaFace dataset as part of a graduate course on Hierarchical Algorithms and Deep Learning.

Research in Industrial Projects for Students (RIPS) **Summer 2017**

Conducted undergraduate research with a team at the University of California Los Angeles for Lawrence Livermore National Laboratory. Created a mathematical model to predict the state variables of hot, dense plasmas that was less computationally expensive than molecular-level simulations, but more accurate than existing statistical models.

Mathematics Advanced Study Semesters (MASS) **Fall 2016**

Participated in a semester-long intensive program run by the Department of Mathematics at the Pennsylvania State University, taking two higher-level courses in the areas of Algebra and Analysis: *Hypercomplex Numbers* and *Approximation of Functions and Applications*. Completed research for final projects on the subjects of crystallographic

groups and linear programming with the simplex method.

REU through the Mathematical Biosciences Institute (MBI) **Summer 2016**

Conducted research at Indiana University Purdue University Indianapolis with Dr. Julia Arciero in collaboration with Dr. Giorgio Raimondi from Johns Hopkins School of Medicine through a program at the Mathematical Biosciences Institute at The Ohio State University. Developed an experimentally based theoretical model for transplant rejection in order to predict the effect of the adoptive transfer of regulatory T-cells on a transplant graft.

Presentations & Posters

Equations of State for Matter at Extreme Conditions

Nebraska Conference for Undergraduate Women in Mathematics — January 2018

Joint Mathematics Meetings in San Diego, California — January 2018

59th Annual Meeting of the APS Division of Plasma Physics in Miwaukee, Wisconsin — October 2017

Using a Theoretical Model to Predict Transplant Rejection

Mathematical Biosciences Institute Capstone Conference — August 2016

Indiana Undergraduate Math Research Conference — August 2016

Extracurricular Activities

Math Tutor through Penn State Learning **2016-present**

Led one-on-one tutoring, group sessions, and large exam reviews for introductory math classes.

State of State **2015-present**

Content Director 2017-present

Directed and served on the Content Committee to choose and prepare student, faculty, and community speakers for the annual State of State conference held in February.

THON Volunteer **2014-present**

Dancer Relations Committee 2016-present

Rules and Regulations Committee 2014-2016

Volunteered yearlong to provide for the health and safety of students participating in THON, a 46 hour no-sitting, no-sleeping dance marathon that raises money for the children and families impacted by childhood cancer.

Polish Student Organization **2016-present**

Vice President 2016-2017

Presided over weekly meetings and planned monthly events in order to create a cultural learning experience.

Meet the Professor Club **2015-2016**

Vice President, Treasurer 2015-2016

Organized weekly lunches in order to facilitate conversation between students and faculty in the Chemistry, Biology, and Biochemistry Departments.

SHOTIME Orientation Mentor **2015-2016**

Served as an orientation mentor for incoming freshman to the Schreyer Honors College for two years.

Awards & Honors

Dean's List Fall 2014, Spring 2015, Spring 2016

S.T.A.R.T. Diversity Award, 1^{st} Place Spring 2016

Academic Excellence Scholarship 2014-present

University Park Four Year Provost Fund 2014-present

Skills

MATLAB

Solving systems of differential equations

Performing numeric analyses on large-scale systems

Python

Scientific computing libraries: numpy, scipy

Deep learning with Tensorflow and Pytorch

Experience with C++ and Java

LaTex

Leadership: Took the initiative to become heavily involved in organizations on campus, was instrumental in organizing and planning large events, and gained experience directing others.

Communication: Experience communicating with individuals from various academic backgrounds from participating in interdisciplinary research and tutoring.